REPORT DOCUMENTATION PAGE

Form Approved
OMB No. 0704-0188

1. REPORT DATE *(DD-MM-YYYY)*	**2. REPORT TYPE**	**3. DATES COVERED** *(From - To)*
22 August 2016	Master's Thesis	01 August 2016 – 31 August 2016

4. TITLE AND SUBTITLE
Polyhedral Oligomeric Silsesquioxane (POSS) Dianiline as a Replacement for Toxic Methylenedianiline in PMR-15: Chemistry and Properties

5a. CONTRACT NUMBER

5b. GRANT NUMBER

5c. PROGRAM ELEMENT NUMBER

6. AUTHOR(S)
Jason T. Lamb

5d. PROJECT NUMBER

5e. TASK NUMBER

5f. WORK UNIT NUMBER
Q16J

7. PERFORMING ORGANIZATION NAME(S) AND ADDRESS(ES) AND ADDRESS(ES)

Air Force Research Laboratory (AFMC)
AFRL/RQRP
10 E. Saturn Blvd.
Edwards AFB, CA 93524-7680

8. PERFORMING ORGANIZATION REPORT NO.

9. SPONSORING / MONITORING AGENCY NAME(S) AND ADDRESS(ES)

Air Force Research Laboratory (AFMC)
AFRL/RQR
5 Pollux Drive
Edwards AFB, CA 93524-7048

10. SPONSOR/MONITOR'S ACRONYM(S)

11. SPONSOR/MONITOR'S REPORT NUMBER(S)
AFRL-RQ-ED-OT-2016-255

12. DISTRIBUTION / AVAILABILITY STATEMENT
Approved for Public Release; Distribution Unlimited. The U.S. Government is joint author of the work and has the right to use, modify, reproduce, release, perform, display, or disclose the work. PA Clearance Number: 16402 Clearance Date: 8/17/2016

13. SUPPLEMENTARY NOTES
For presentation at North Carolina State University; thesis submitted to the Graduate Faculty of North Carolina State University in partial fulfillment of the requirements for the degree of Masters of Science
Prepared in collaboration with ERC

14. ABSTRACT
With the goal of replacing methylene dianiline (MDA) in PMR-15 (polymerizable monomeric reactant), which is a known toxin to humans, a thermally stable, polyhedral oligomeric silsequioxane (POSS) dianiline, which features an aromatic periphery, was copolymerized as a "drop-in" replacement. The chain length of the experimental oligomers was varied to study effects of cross-link density and nadic endcap concentration. The resultant oligomers were characterized for various neat resin and composite properties. The POSS dianiline has shown previously in 6-FDA-ODA-PEPA type polyimides to improve moisture resistance and processability. It was shown that the bulky monomer addition improved moisture resistance (80% decrease in ultimate moisture absorption) and processability (uncured Tg and rheology) were improved. Uncured Tg values decreased by as much as 85°C and complex viscosity decreased by 3 orders of magnitude. Viscosity is low enough that resintransfer molding (RTM) is possible. However, thermal properties such as glass transition temperature (Tg) and long-term thermal oxidative stability (TOS) along with composite strengths were hindered. Shortening the chain length, which increases cross-link density is shown to improve cured Tg and can be manipulated. The decreased chain length causes increased nadic endcap concentration which has been shown to lower the thermal stability of the polyimide.

15. SUBJECT TERMS
N/A

16. SECURITY CLASSIFICATION OF:			**17. LIMITATION OF ABSTRACT**	**18. NUMBER OF PAGES**	**19a. NAME OF RESPONSIBLE PERSON**
					A Guenthner
a. REPORT	**b. ABSTRACT**	**c. THIS PAGE**	SAR	79	**19b. TELEPHONE NO** *(include area code)*
Unclassified	**Unclassified**	**Unclassified**			N/A

Standard Form 298 (Rev. 8-98)
Prescribed by ANSI Std. 239.18

LAMB, JASON THOMAS. Polyhedral Oligomeric Silsesquioxane (POSS) Dianiline as a Replacement for Toxic Methylenedianiline in PMR-15: Chemistry and Properties. (Under the direction of Dr. C. M. Balik.)

With the goal of replacing methylene dianiline (MDA) in PMR-15 (polymerizable monomeric reactant), which is a known toxin to humans, a thermally stable, polyhedral oligomeric silsequioxane (POSS) dianiline, which features an aromatic periphery, was co-polymerized as a "drop-in" replacement. The chain length of the experimental oligomers was varied to study effects of cross-link density and nadic endcap concentration. The resultant oligomers were characterized for various neat resin and composite properties. The POSS dianiline has shown previously in 6-FDA-ODA-PEPA type polyimides to improve moisture resistance and processability. It was shown that the bulky monomer addition improved moisture resistance (80% decrease in ultimate moisture absorption) and processability (uncured T_g and rheology) were improved. Uncured T_g values decreased by as much as 85°C and complex viscosity decreased by 3 orders of magnitude. Viscosity is low enough that resin-transfer molding (RTM) is possible. However, thermal properties such as glass transition temperature (T_g) and long-term thermal oxidative stability (TOS) along with composite strengths were hindered. Shortening the chain length, which increases cross-link density is shown to improve cured T_g and can be manipulated. The decreased chain length causes increased nadic endcap concentration which has been shown to lower the thermal stability of the polyimide.

Polyhedral Oligomeric Silsesquioxane (POSS) Dianiline as a Replacement for Toxic Methylenedianiline in PMR-15: Chemistry and Properties

by
Jason Thomas Lamb

A thesis submitted to the Graduate Faculty of
North Carolina State University
in partial fulfillment of the
requirements for the degree of
Masters of Science

Materials Science and Engineering

Raleigh, North Carolina

2016

APPROVED BY:

Dr. Orlin Velev	Dr. Thomas LaBean

Dr. C. Maurice Balik
Committee Chair

BIOGRAPHY

Jason Lamb was born on September 15, 1982 in Columbia, SC. He grew up in Garner, NC just outside of Raleigh, NC. In 2005, he received a B.S. in Mathematics from N.C. State University. After working in the restaurant industry off and on for 10 years and at Credit Suisse for 2.5 years, he went back to school in May, 2010. Two years later, he received a B.S. in Materials Science and Engineering. During this time, he served as an undergraduate research assistant under the advisement of Dr. CM Balik. In July, 2012 he began work as a process engineer for Acucote, Inc. in Graham, NC. In this role, he was tasked with process improvement on one silicone coating line, two adhesive coating and lamination lines and five slitter/winders. In January 2014, he started in his current role as a materials research engineer for ERC, Inc. The position is located at Edwards AFB, CA at the Air Force Research Laboratory and he is currently living in Lancaster, CA. The position is in the Advanced Materials Group, currently lead by Dr. Andrew Guenthner. The group is in the rocket propulsion division of the aerospace systems directorate. The research focuses of the group include propellant binder development, low surface energy surfaces, high temperature resin systems and low density solid rocket motor components. Jason began working on a master's degree in materials science and engineering in January 2015 by taking online courses through the engineering online program at N.C. State University while conducting research for his thesis at the Air Force Research Laboratory.

ACKNOWLEDGMENTS

I would like to thank several people who made this work possible. First, Dr. Gregory Yandek at the Air Force Research Laboratory (AFRL) who conceptualized, proposed and oversaw the research. Without him, the research would have never taken place. I would also like to thank the other members of the Applied Materials Group at AFRL for their insights and assistance throughout the project.

Secondly, I would like to thank Dr. C. M. Balik at North Carolina State University. He served as my advisor during the project and helped immensely during the writing of this thesis. Moreover, as my professor in my first course on polymers and as undergraduate research advisor, inspired me to seek out a career in polymer research. He was also instrumental in allowing me to pursue a thesis-based master's degree while living in California and taking courses online.

My gratitude also goes to the Strategic Environmental Research and Development Program (SERDP) who funded this work. As we all know, without the funds, the work cannot be done.

Lastly, I would like to thank my fiancé, whose support and patience never wavered during many trying times and late nights.

TABLE OF CONTENTS

LIST OF TABLES

LIST OF FIGURES

Chapter 1: Introduction

Polyimide materials are an important class of polymers which are characterized by high thermal and thermo-oxidative stability, excellent mechanical, electronic and adhesive properties, film- and fiber-forming ability and non-flammability. There are two main types of polyimides that are available commercially: thermoplastic polyimides, which are derived from a condensation reaction between anhydrides and diamines and cross-linked polyimides, which are derived from an addition reaction between imide oligomers. Cross-linked polyimides carry reactive end groups such as nadics, vinyls, acetylenes or phenylethynyls. These imide oligomers are also derived from similar condensation reactions as their thermoplastic counterparts, but the polymer or network formation stems from the addition reaction between the reactive end groups (Scola 1998).

There are many different types of polyimides produced by industry that have trade names such as Kapton®, Vespel®, Avimid N®, Skybond® or Ultradel^{TM} to name a few. Several polyimides have been developed by the aerospace industry at NASA, the U.S. Air Force Research Laboratory and other private firms such as PMR (Polymerized Monomeric Reactants)-II, AFR (Air Force Resin) 700B and PETI (Phenylethynyl Terminated Imide)-5. The applications of polyimides are wide ranging. In the electronics industry, polyimides are used as flexible circuits, flexible connectors, chip carriers and interconnects. In aerospace, polyimides find themselves in wire insulation, motor windings, electrical switches, structural adhesives, etc. They even have a home in the medical industry as used in pacemakers and eye lens implants.

This study is focused on one particular thermosetting polyimide, PMR-15. The 15 in its name is a nod to the average molecular weight of the oligomer of 1,500 g/mol. The material

was developed in the 1970's at NASA's Lewis Research Center as a protective coating, but the high thermal stability was quickly noticed. Ferro Corporation and ICI Fiberite applied PMR-15 to a few sections of aircraft structures and engine components as a composite resin. Over time, confidence in the material grew and the number of applications increased (PMR-15 Polyimide Resin 2016). Current uses in the aerospace industry as a state-of-the-art resin in high-temperature composites include engine bypass ducts, nozzle flaps, bushings and bearings (Polyimide Boosts 2016). The most widely used current application is in GE Aviation's F/A-18E/F and EA-189G engines, where the F414 Outer Bypass Duct is composed of PMR-15 composites. An estimated 20,000 lbs or more of PMR-15 are manufactured each year, with the majority of it being used in aircraft production programs (EEWSA 2016).

PMR-15 is composed of three monomers: 3,3',4,4'-Benzophenonetetracarboxylic dianhydride (BTDA), 5-norbornene-2,3-dicarboxylic anhydride (or nadic anhydride, NA) and 4,4'-methylenedianiline (MDA). The reaction scheme is give in figure 1. The synthesis begins with esterification of the anhydrides in methanol (MeOH). The anhydrides are not initially soluble in MeOH, however, when refluxed, the anhydrides convert to ester acids and become soluble. Upon cooling, MDA is added to the mixture to form oligo (amic acids). The solvent is then evaporated and a yellow powder is left. A thermal treatment closes the rings in the backbone and water and methanol are evolved leaving behind oligoimides. This is the preform of the final product. Processing treatments can be slightly varied at this point depending on the final product, but heat and pressure are typically applied to activate the nadic end caps and cross-link to form a network.

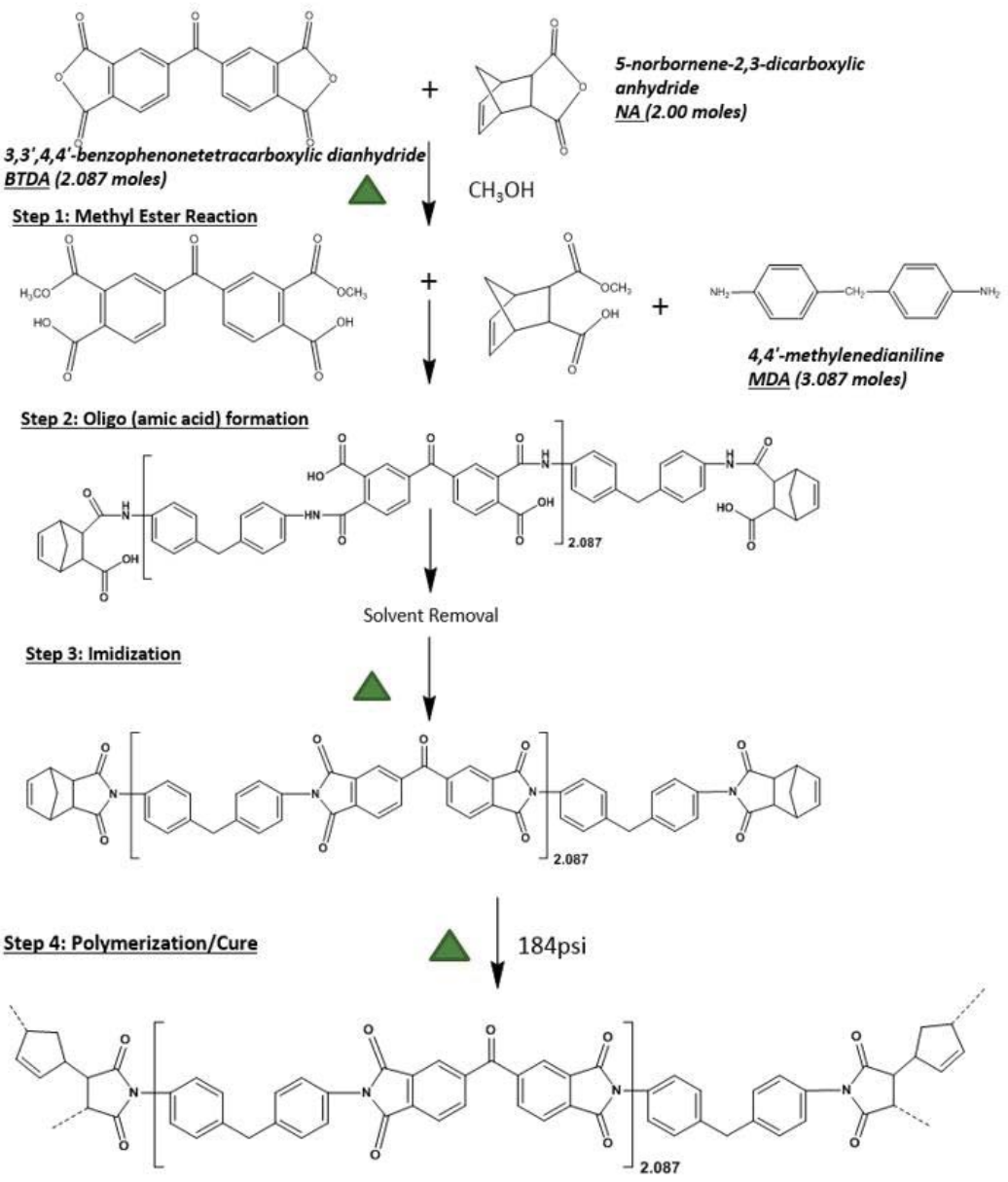

Figure 1. Molecular structures for monomers and reaction scheme with cure for PMR-15.

Unfortunately, since the early 1980's, it has been known that MDA poses health risks and is under heavy scrutiny from organizations such as the Environment, Safety and Occupational Health (ESOH) office of the Air Force. The dangers associated with working with MDA have been widely studied and are well known. Cytochrome P450 (CYP) is a class

of enzyme in the human body which is used to oxidize organic chemicals in the body and liver (Guengerich 2008). CYP activates MDA to form nitroso compounds via N-oxidation which are then converted to nitrosamines, a class of compounds that are known to be highly toxic (Yun 1992, Siraki 2002). Also, intermediate compounds can form an elimination product that conjugates with glutathione, depleting the oxygen free radical scavenger concentration which protects DNA from degradation leading to cancer (Scholz 1989, Hughes 1964, Kopelman 1966).

The Occupational Safety and Health Administration (OSHA) has set occupational exposure limits to MDA of short-term exposure to 100 parts per billion (ppb) and an eight-hour time-weighted average to 10 ppb (Occupational Exposure 1992). The costs associated with production of PMR-15 have increased because of handling requirements of the dangerous compound. Many companies have gone away from use of PMR-15 in manufacturing due to the increased costs and potential liability. A design engineer (Leslie Kalmbach) at Lockheed Martin Skunk Works in Palmdale, CA, has stated that the use of PMR-15 has been eliminated in their production. There are resins available for use for lower service temperatures such as bismaleimides, and for higher service temperatures, such as AFR-PE. However, the use of a mid-service temperature resin such as PMR-15 has been inhibited due to these health concerns. This has had a significant impact on design for aerospace applications. A solution to this problem is sorely needed. A non-toxic resin with similar properties to PMR-15 would help to reduce cost for and liability of manufacturers.

The aim of this work is to develop a replacement for MDA in PMR-type resins. There have been upwards of 50 different amines studied as alternatives, but none of which have been

able to match all of the beneficial properties of PMR-15 (Chuang 2002). The different approaches taken and resulting properties will be discussed in chapter 2.

In contrast to the known documented approaches to developing an aniline to replace MDA, this work consists of using a silsesquioxane-based dianiline monomer with a silicon-oxygen core and aromatic, thermally stable organic periphery. A polyhedral oligomeric silsesquioxane (POSS) dianiline was initially synthesized for incorporation into Kapton-like polyimides, which exhibited good resistance to oxygen flux for use in low-earth orbit applications (Vij 2012). Kapton films are used as thermal insulators on the exterior of spacecrafts and when exposed to atomic oxygen experience severe degradation leading to reduced spacecraft lifetimes (Tomczak 2005). The work demonstrated that nano-dispersed POSS cages within the polyimide matrix reacted with the atomic oxygen to produce a thin siliceous layer that acts like a passivation layer to prevent further oxidation of the polymer matrix. Figure 2 shows the reaction scheme from a commercially available phenyl-POSS tetrasilanol to a mixture of cis- and trans- phenyl-POSS dianiline.

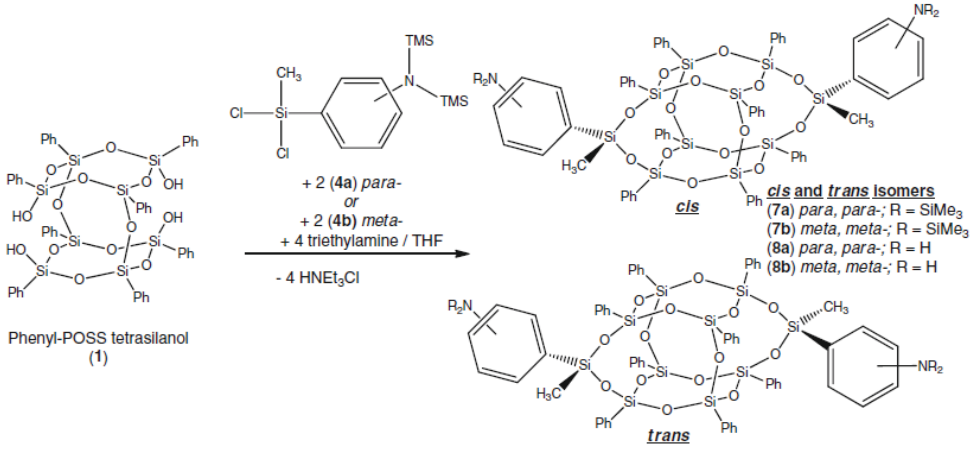

Source: Vij 2012

Figure 2. Scheme illustrating the synthesis of cis- and trans- phenyl-POSS dianilines derived from tetrasilanol.

This group from the Air Force Research Laboratory at Edwards Air Force Base in California also used this POSS dianiline to covalently bond into the backbone of 6-FDA-ODA-PEPA (Pinson 2013), which is a polyimide with phenylethynyls end groups. The starting monomers of the polyimide are composed of 4,4'-(hexafluoroisopropylidene) dipthalic anhydride (6-FDA), 4,4'-diaminodiphenyl ether (or oxygen dianiline, ODA) and phenylethynylphthalic anhydride (PEPA). The POSS dianiline was used as a direct replacement of ODA in the oligomer chemistry on an average of 1 and 3 units per chain. The control material has 5 equivalents of ODA per chain as the degree of polymerization is 4 on average. Therefore, in all cases, ODA was not completely replaced by POSS. Figure 3 shows the synthesis scheme of these reactions.

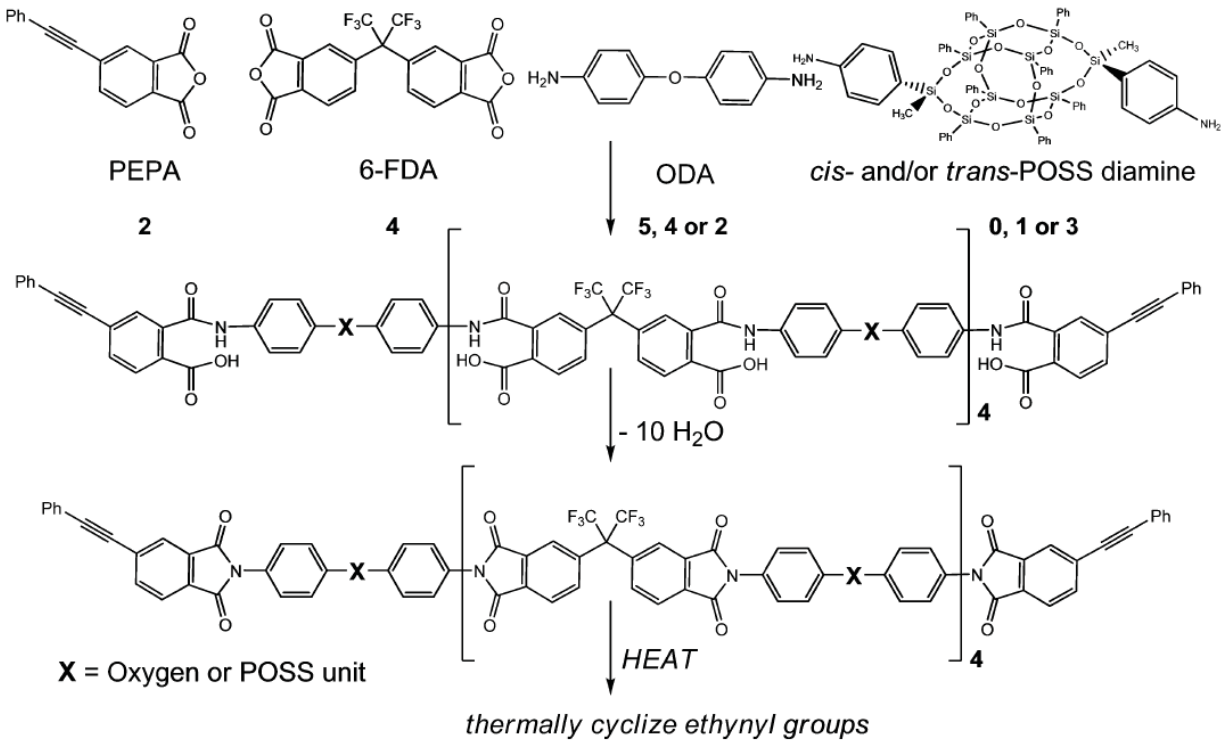

Source: Pinson 2013

Figure 3. General synthesis scheme of phenylethynyls-terminated POSS-containing oligoimides with and average degree of polymerization of four.

The promising results were threefold: (1) viscosity of the uncured oligomers was reduced, (2) thermal stability from thermogravimetric analysis (TGA) was improved and (3) moisture resistance was improved. Each improvement was increased by the increased POSS content. However, glass transition temperature (T_g) was reduced significantly in the cured state. The charts representing these findings are found below in figure 4.

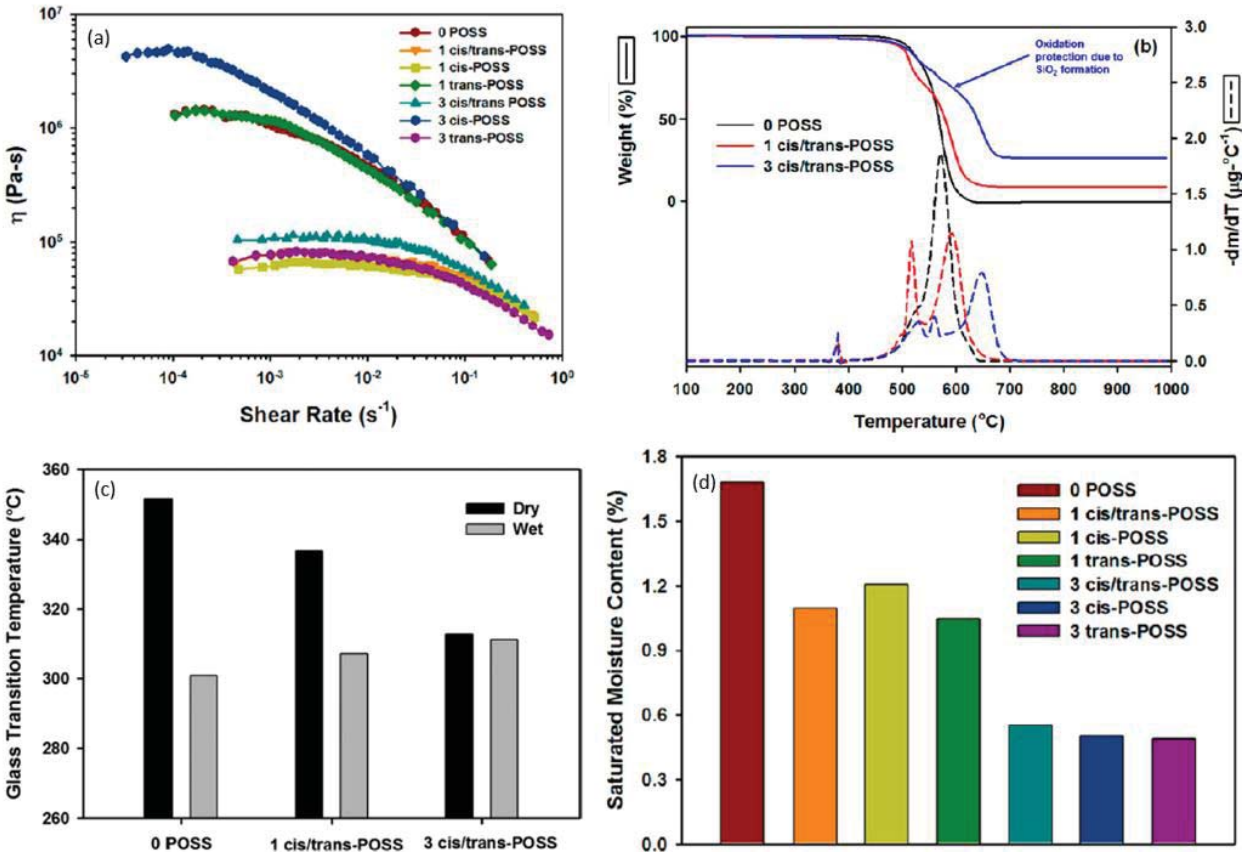

Figure 4. Resin characterization from the work of Pinson et al.: (a) rheology – viscosity as a function of shear rate, (b) TGA measurements, (c) dry and wet T_g measurements from DSC and (d) total moisture content at saturation.

As seen in figure 4 (a), POSS co-oligomerization reduced the zero-shear viscosity for the majority of the oligomers. However, in the 1 trans- and 3 cis- cases, the viscosity was equal to or higher than the control. Further studies were done to decouple the storage and loss moduli

by performing complex viscosity experiments. It was shown that different isomers of the POSS dianiline incorporated into the oligomers affected linearity of the oligomers and inter-chain interactions. The cis/trans mixtures had the lowest degree of order and interactions, therefore consistently resulted in lower viscosities. The figure also shows that the 3 cis/trans- mixture had an even lower viscosity than did the 1 cis/trans- mixture.

In the TGA plot of figure 4 (b), it is clearly seen that the POSS containing samples exhibit a higher char yield than the control. The 1-cis/trans-POSS begins to lose mass at an earlier temperature than either of the other two, but the protection due to SiO_2 formation begins to take over and eventually out-performs the control. With the 3-cis/trans-POSS sample, the initial mass loss even begins at the same time as the control, and then the SiO_2 formation gives the material even higher thermal stability. The isomer effect that was seen in the rheological experiments was not evident.

Perhaps the greatest result is the reduction in moisture uptake. Figure 4 (d) shows the moisture mass gained as a percentage of initial mass when fully saturated. Here, both the effect of POSS concentration and isomer type are shown. Clearly, the amount of POSS included in the imide backbone directly affects moisture uptake. The 1-POSS samples absorb about two-thirds that of the control and the 3-POSS materials absorb only about one-third. There are small differences in the isomer type at the same POSS amount, but the differences are minimal.

The downside to POSS incorporation is the cured T_g values. Figure 4 (c) shows these in graph form. The T_g values decrease approximately 20 °C for 1-POSS and about 45 °C for 3-POSS when they are dried. Again, the isomer has a negligible effect on T_g. In continued research, yet unpublished, it has been shown that reducing the degree of polymerization can

counter the T_g decrease by way of increasing cross-link density while maintaining the positive results from POSS incorporation.

This work is the source of inspiration for investigating POSS dianiline as a suitable replacement for MDA in PMR-15. If POSS dianiline can be successfully incorporated into the chemistry of PMR-15, one would expect to find similar results as with the phenylethynyl end capped polyimides. To offset the decrease in T_g that is expected, oligomers with varying chain lengths can be synthesized to see if the thermal properties of PMR-15 can be matched. Other properties such as processability and moisture resistance would be expected to be improved.

Chapter 2: Literature Review and Program Framework

2.1 MDA Replacement

Efforts to replace MDA with other, non-toxic anilines have been ongoing since the early 1980's. Many of these efforts have been successful and have led to commercialization of a number of oligomers developed by NASA; however none have exhibited equivalent properties of PMR-15. Kathy Chuang at NASA catalogued over 40 such anilines and her findings are listed in table 1-4 below (Chuang 2007).

Table 1 lists many dianilines with BTDE (the methyl ester of BTDA) and 4,4'-(hexafluoroisopropylidene) diphthalic ester (HFDE). As BTDE is the direct comparison to PMR-15, only those results will be discussed. When the methylene bridge of MDA is changed by adding a phenyl group, replacing with a carbonyl or sulfur, the themo-oxidative stability (TOS) of the resin is comparable to that of PMR-15. However, the T_g is greatly reduced. Interestingly, when a sulfone group is the bridge between the two anilines and the amines are para- to the bridge, the T_g is almost exactly the same as PMR-15 (yet with poor TOS). With the same bridge and the aniline groups placed ortho- to the sulfone, the TOS is reduced but the T_g is also reduced by almost 50 °C. When the bridge is removed altogether as with p-phenylenediamine (PDA), the T_g is significantly increased, but conversely the TOS is reduced. The same is true when longer carbon chains are used as the bridge, as with ethylene, ethane and cumulene bridges. Even when cyclic groups replace the bridge, a similar result of high T_g and low TOS occurs.

A few trends can be seen from these results. The TOS of these polyimides increased with decreasing aliphatic content which occurs by reducing the aliphatic nadic endcap

percentage. Diamines with benzylic linkages (-CH_2-, -CHPh) between the phenyl rings such as MDA and diaminotriphenyl methane (DAPTM) result in better TOS. Also, non-carbon linkages like sulfur and oxygen reduce the T_g.

Table 1. Characterization of PMR Polyimide Resins Based on BTDE and HFDA with the Nadic Endcap (Normalized MW=1500 g/mole)

Diamine Structure	Dianhydride Dimethyl ester	Resin Wt. Loss[b] @316 °C/500 hr (mg/cm^2) (BTDE / HFDE)	Composite Wt. Loss (%)[b] @ 316°C/400 hr (BTDE / HFDE)	T_g (°C) / Resin Postcure in Air[c] @ 316 °C/16 hr (BTDE / HFDE)
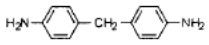	BTDE/HFDE	4.97 / 5.63	1.88 / 1.56	322 / 324
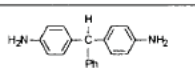	BTDE/HFDE	5.85 / 6.44	1.64 / 1.61	317 / 315
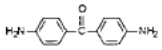	BTDE/HFDE	5.15 / 5.67	---[d] / 2.25	267 / 277
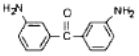	BTDE/HFDE	6.46 / 7.74	2.74 / 2.15	269 / 260
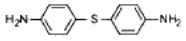	BTDE/HFDE	5.26 / 6.31	2.20 / ---	289 / 302
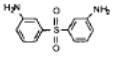	BTDE/HFDE	8.48 / 8.75	6.64 / ---	273 / 262
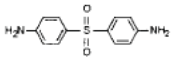	BTDE/HFDE Brittle/Brittle	12.67 / 10.67	-------	322 / 300
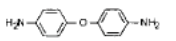	BTDE/HFDE	9.51 / 6.89	3.68 / 1.91	321 / 316
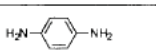	BTDE/HFDE Brittle/ ---	29.52 / 6.41	--- / 1.66	396 / 355
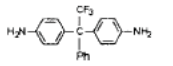	BTDE/HFDE	11.03 / 11.51	3.20 / 2.77	351 / 345
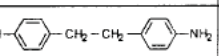	BTDE/HFDE Brittle/ ---	21.69 / 12.34	15.56 / 2.60	360 / 380
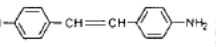	BTDE/HFDE Brittle/ ---	38.76 / 8.12	--- / 10.15	410 / 355
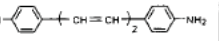	BTDE/HFDE	10.96 /10.96	--- / ---	360 / 375
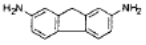	BTDE/HFDE Brittle/ ---	12.69 / 5.16	--- / 2.13	375 / 325
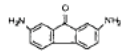	BTDE/HFDE	29.37 / 6.01	--- / 7.51	390 / 350
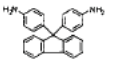	HFDE	--- / 18.83	--- / ---	--- / 373

Source: Chuang 2007

Table 2 shows dianilines with ether, isopropylidene and hexafluoroisopropylidene linkages and two or more phenyl rings between the anilines. The T_g in each case was reduced

as was the TOS with two of the molecules shown. The flexible linkages are the cause of the reduced properties, but provide an enhancement of processability. 3,4'-oxydianiline (ODA) has actually been commercialized as a composite resin in LARC-RP-46 and is patented (Pater 1992).

Table 2. Properties of PMR-15 Analogs

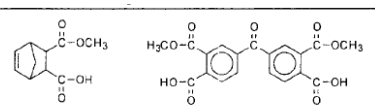

NE BTDE MDA

Diamine Structure	Diamine	n	T_g[b] (°C)	Composite Weight Loss (%)[c] @288°C/1400 hr
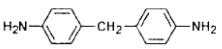	MDA	2.087	345	1.52
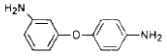 (RP-46)	3,4′-ODA	2.087	270	4.74
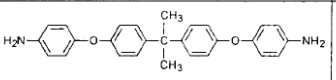	BAPP	2	280	5.0
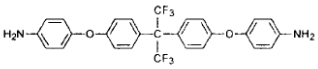	BDAF	2	297[d]	---
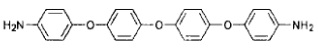	BDAO	2	278[d]	---
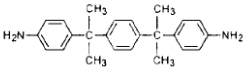	Bisaniline P	2	309[e]	---
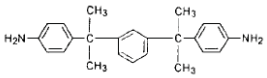	Bisaniline M	2	286[e]	---

Source: Chuang 2007

Table 3 shows dianilines that all have three phenyl rings in the chain with either methylene or carbonyl linkages between them. The methylene proved to be more thermally stable than the carbonyl as evidenced by the TOS data. Conversely, the carbonyl linkages yielded higher T_gs than the methylene bridges. The table also shows similar anilines with meta- and para- placement of the amines. When both amines were placed in the para- position, the

T_g was higher and the TOS was also better performing than when meta- positions were used. The poorest results were when both amines were in the meta- position.

Table 3. Properties of PMR-15 Analogs Containing 3-Ring Diamines.

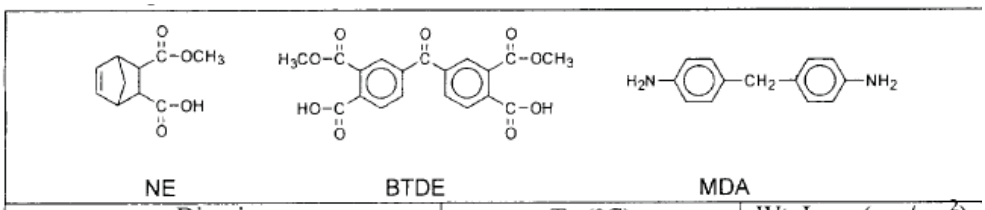

NE BTDE MDA

Diamine	T_g (°C) No postcure	T_g (°C) Postcure[b]	Wt. Loss (mg/cm^2) 3024 h @ 288°C
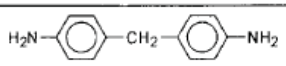	299	333	13.6
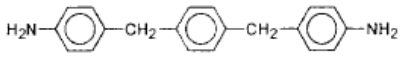	268	328	13.2
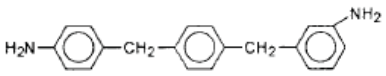	246	316	14.0
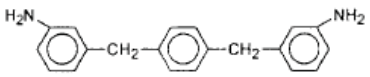	239	278	15.6
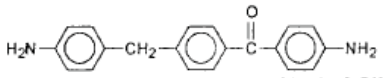	272	332	16.0
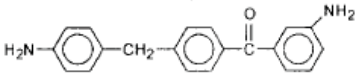	249	319	17.0
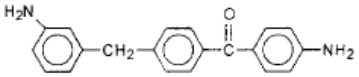	252	321	17.2
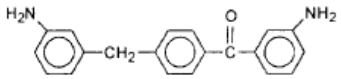	243	298	18.5
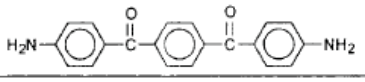	288	401	---[c]
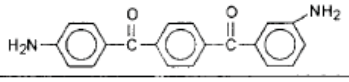	269	378	---[c]
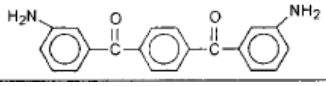	267	345	---[c]

Source: Chuang 2007

Table 4 shows anilines with four phenyl rings in the chain. Each one has either a methylene or carbonyl between the phenyl rings with one amine and either a methylene, sulfur

or ether linkage on the opposite end of the molecule. The methylene and carbonyl linkages on the ends had higher performing TOS than the sulfur analogs. These more flexible (due to the number of linkages) four ring chains all exhibit lower T_gs than the three ring counterparts from table 3.

Table 4. Properties of PMR-15 Analogs Containing 4-Ring Diamines.

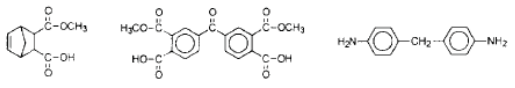 NE BTDE MDA			
Diamine	T_g (°C) No postcure	T_g (°C) Postcure[b]	Wt. Loss (mg/cm^2) 3024 h @ 288°C
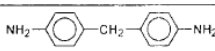 **MD**	299	329	11.7
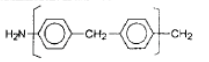 ***p*-MM**	225	301	12.0
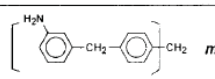 ***m*-MM**	202	253	13.4
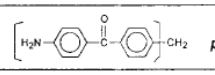 ***p*-CM**	228	315	14.4
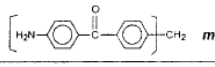 ***m*-CMC**	205	293	16.1
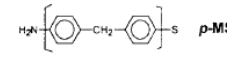 ***p*-MS**	217	318	13.2
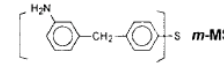 ***m*-MS**	210	261	14.7
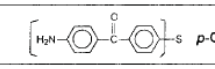 ***p*-CS**	227	323	14.9
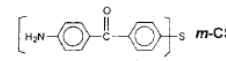 ***m*-CS**	203	276	18.1
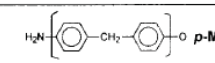 ***p*-MO**	225	314	18.0
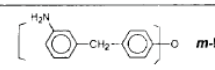 ***m*-MO**	203	270	19.2
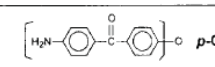 ***p*-CO**	232	321	19.4
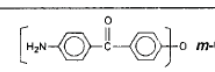 ***m*-CO**	209	271	21.1

Source: Chuang 2007

2.2 POSS Background

The name says it all when it comes to describing a polyhedral oligomeric silsesquioxane (POSS) unit. Silsesquioxane is a generic term for a siloxane molecule that has a generic formula $(RSiO_{1.5})_n$ (Silsesquioxanes 2001). Each silicon atom is bonded with one and a half (sesqui) oxygen atoms on average. The term oligomeric refers to the number of units that are repeated and is from the term oligomer where oligo- means "few" and –mer means "units." Therefore, there are few repeat units in an oligomer. The polyhedral term refers to the geometrical shape of the molecule. A polyhedral molecule must have a three-dimensional shape and occurs in a closed geometrical pattern. Thus, POSS is a molecule which has few repeat $SiO_{1.5}$ units and occurs in some sort of geometrical shape.

POSS molecules contain an inner inorganic framework as described above and also can be bounded on the exterior by inert and/or reactive organic substituents (Pan 2007). An example of the structure for a POSS unit with 8 silicon atoms is shown in figure 5. In the figure, the R groups represent the inert substituents and the X group is a reactive one. This is a simplified picture of what a POSS molecule can look like. The R groups can represent any number of substituents, from purely aliphatic chains to phenyl groups to crystalline fluoro-alkyl chains. Also, any number of the substituents can be reactive depending on the synthesis methods. The reactive substituents allow for the POSS molecule to be further functionalized to enhance miscibility in a solvent or to be bonded to polymeric chains through copolymerization or grafting.

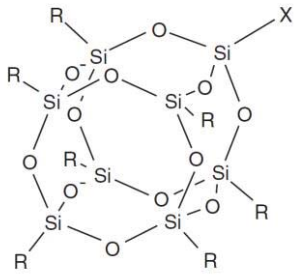

Source: Pan 2007

Figure 5. Schematic Structure of POSS.

POSS was invented by Donald Scott at General Electric Company in 1946 (Scott 1946). During the 1990's, rapid development in the field occurred at the University of California-Irvine with the Feher group and at the Air Force Research Laboratory with the Lichtenhan group. The Feher group developed methods for synthesizing and chemically modifying many structurally well-defined Si/O frameworks. The Lichtenhan group developed many polymer-related applications through the use of discrete POSS molecules. Today, many POSS reagents with a number of different functionalities are available from Hybrid Plastics out of Hattiesburg, Mississippi.

Depending on the number and location of functional groups on the POSS cage, different architectures of POSS co-polymerization can occur. Figure 6 below depicts several such architectures. Polymers such as polysiloxane, poly (methyl methacrylate), poly (4-methylstyrene, polynorbornene, polystyrene, polyurethane and thermoplastic polyimides have been studied as copolymers with POSS. Monofunctional and difunctional POSS are commonly used in these cases.

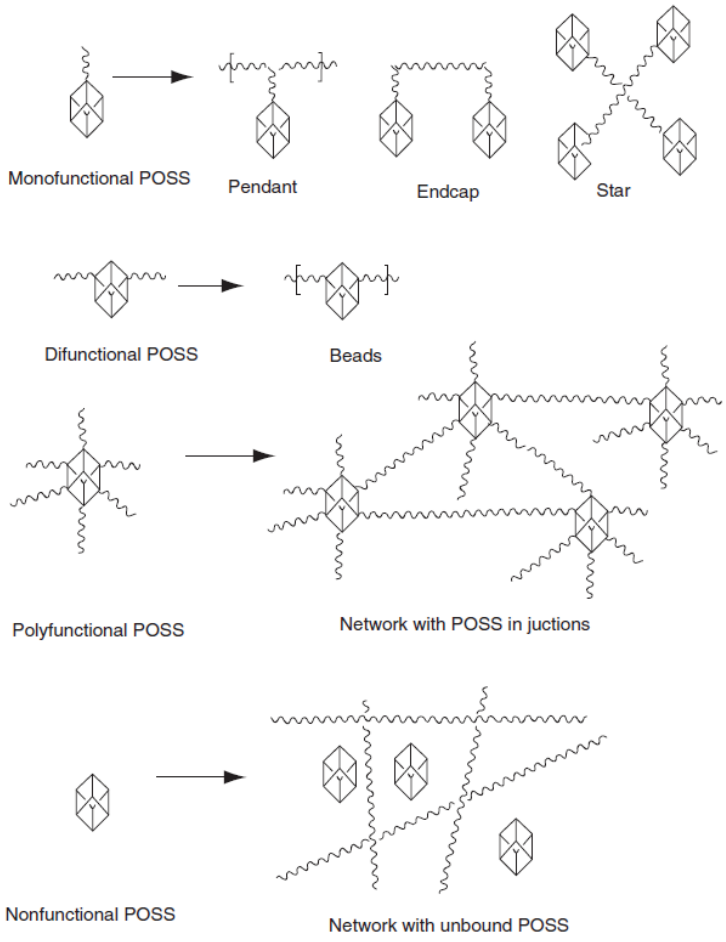

Source: Pan 2007

Figure 6. POSS/polymer architectures.

2.3 Program Framework

2.3.1 SERDP Proposal

In 2012, the Strategic Environmental Research and Development Program (SERDP) released a solicitation for a research plan to solve the MDA toxicity problem with PMR-15. Dr. Gregory Yandek of the Air Force Research Laboratory at Edwards Air Force Base responded to this solicitation and proposed POSS dianiline as a potential replacement for MDA in PMR-15. This research is the basis for the present study.

2.3.2 Research Plan

2.3.2.1 Synthesis

Synthesis of POSS dianiline is described by Vij et al. (Vij 2012). This process delivers a mixture of cis- and trans- POSS isomers which can be isolated. It was shown that isomeric configuration can affect processability, specifically viscosity, but not ultimate properties in the cured state (Pinson 2013). Therefore, isomer isolation was not pursued and the cis/trans mixture was used.

Three varieties of oligomers have been synthesized using the POSS dianiline. First, the POSS dianiline was used as a drop-in replacement for MDA in PMR-15. That is, the stoichiometric ratios of starting materials (BTDA, NA and POSS dianiline) were the same. However, because the POSS monomer is larger than MDA, it will decrease the cross-link density which would expect to reduce T_g. To mitigate this effect, two other oligomers were synthesized which would increase cross-link density. PMR-15 has a degree of polymerization of n=2.083 and the first POSS containing oligomer has a degree of polymerization of n=2. Similar architectures will be used for the other two oligomers to be synthesized, but have degrees of polymerization of n=1 and n=0. Figure 7 below shows the chemical structure of the three experimental oligomers to be synthesized. Details of the synthesis procedure are given in chapter 3.

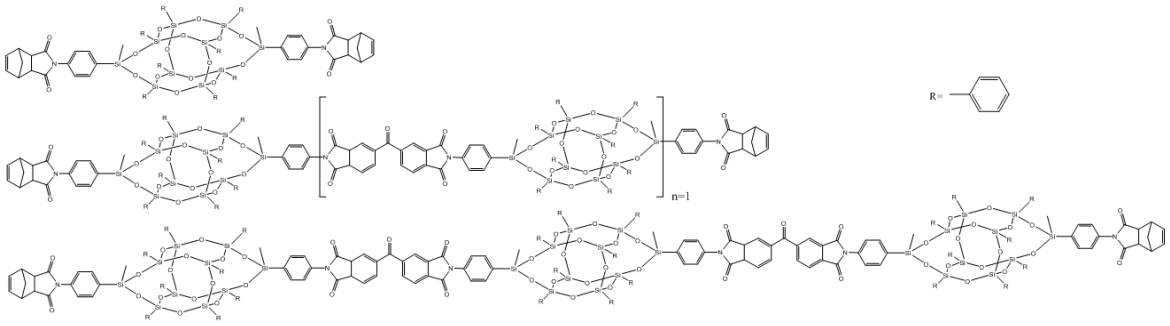

Source: Yandek 2013

Figure 7. Target PMR oligomers featuring NA, BTDA and POSS dianiline substituted for MDA with varying repeat units n(POSS-BTDA); n=0 (top), n=1 (middle) and n=2 (bottom).

2.3.2.2 Resin Characterization

Several critical properties of the neat resins were characterized for comparison with PMR-15. Although an extensive database exists for properties of PMR-15, it was also synthesized and characterized for direct comparison. In general, the experimental polymers that exhibit a reduction of 5% in any of the key properties were eliminated as potential candidates. Conversely, polymers that meet or exceed the properties of PMR-15 were fabricated into carbon fiber composites and further characterized as described in the next section.

Initially, the oligomers were characterized for their chemical makeup by nuclear magnetic resonance (NMR) spectroscopy. Viscosity characteristics were measured by parallel plate rheometry. This is an important property because it directly affects processability of the resin. Thermal properties of the resin were measured by differential scanning calorimetry (DSC), thermogravimetric analysis (TGA) and thermomechanical analysis (TMA). The T_g was a key property when selecting the polymer for further composite characterization. Thermo-

oxidative stability (TOS) was measured by TGA as well as isothermal aging of compression molded discs of neat resin. Lastly, moisture uptake was measured by submerging the neat resin discs in boiling water and measuring mass increase over time.

2.3.2.3 Composite Fabrication

Flat laminate composite panels of PMR-15 and down-selected oligomers of size 4x4x0.1 (in.) were fabricated with Toray T650-35, 8 harness satin weave, carbon fiber mesh. Solutions of the oligomers in the amic acid state and methanol were made and painted onto each carbon fiber fabric ply, then partially dried to allow for handling. Each ply was stacked in a steel compression mold to the desired part thickness and cured under pressure in a hot press. A known cure cycle for PMR-15 has been well established, but for new oligomers an appropriate cure cycle was determined. The flat laminate was then removed from the mold and sectioned into the appropriate coupon geometry for each test method.

2.3.2.4 Composite Characterization

Composite constituent component data of each panel was ascertained according to ASTM D3171. Flexural and short beam shear (SBS) mechanical data was gathered using a Tinius Olsen mechanical tester. Flexural strength and modulus was determined in accordance with ASTM D7264 and short beam shear strength will be determined by ASTM D2344. TOS of the composite coupons was determined in the same method as with neat resin discs.

Again, the threshold properties for the composite panel fabricated from the down selected resin system were used as criteria to warrant follow-on work following this effort. The threshold for composite properties was also within 5% of the control material.

Chapter 3: Experimental

3.1 Materials

Methanol (MeOH) and tetrahydrofuran (THF) were obtained from Fischer Scientific and were used as received. 3,3,',4,4'-benzophenonetetracarboxylic dianhydride and 5-norbornene-2,3,-dicarboxylic anhydride were obtained from Sigma-Aldrich and used as received and stored in a dry, N_2-environment glove box. 4,4' methylene dianiline was also obtained from Sigma-Aldrich and was also used as received. IM7 4 harness satin weave carbon fiber fabric was used as received from Hexcel. Polyhedral oligomeric silsesquioxane (POSS) dianiline was synthesized by Dr. Tim Haddad at the Air Force Research Laboratory at Edwards Air Force Base, CA. The procedure has been previously reported (Vij 2012).

3.2 Poly (amic acid) synthesis and imidization

PMR-15 (5g scale)

In a dry, N_2-environment glove box, 2.0155g 3,3,'4,4,'-benzophenonetetracarboxylic dianhydride (BTDA) and 0.9850g 5-norbornene-2,3-dicarboxylic anhydride (NA) were added to a 50mL round-bottomed flask. The flask was removed and 17mL methanol (MeOH) was added. The mixture was stirred and refluxed for 2 hours, during which time the powders dissolved and the solution became yellow and clear. The solution was cooled to room temperature (RT), for approximately 2 hours. 1.836g of 4,4' methylene dianiline (MDA) was added and stirred for 1 hour. The MDA dissolved after approximately 5 minutes, at which time the solution became a darker yellow/amber color. Then, the solvent was evaporated using a Rotovap and 5.2177g of a bright yellow amic acid powder was recovered.

To thermally imidize, 4.27g of the amic acid was placed into a 200°C oven for 2 hours, then 230°C for 30 minutes. 3.65g of brown imide powder was recovered.

PMR-15-THF (5g scale)

1.8363g MDA was dissolved into 10mL THF and 2.0159g BTDA was dissolved separately into 70mL THF. The BTDA solution was slowly added to the MDA solution while stirring. The clear solutions became increasingly darker shades of yellow until approximately half of the BTDA solution was added. At that time, white precipitate formed and the solution was a cloudy, pale yellow shade. Then, a solution of 0.9851g NA and 10mL THF was slowly added to the cloudy mixture. There was no obvious change in appearance and was left to stir overnight.

The following day, the solution was discovered to be clear and yellow in color. The solvent was evaporated and 4.1090g bright yellow amic acid powder was recovered. 3.5g of the amic acid powder was placed into a 200°C oven for 2 hours, then 230°C for 30 minutes, to imidize. 3.123g of brown imide powder was recovered.

PMR/POSS N=2 (3g scale)

In a dry N2-environment glove box, three solutions were made: 2.4677g meta/para POSS dianiline with 25mL THF, 0.2023g 5-norbornene-23-dicarboxylic anhydride (nadic) with 2mL THF and 0.3966g BTDA with 4mL THF. While stirring, the BTDA solution was added to the POSS dianiline solution. The solution became yellow and darkened as more solution was added. After 1 hour of stirring, the nadic solution was added and no change in appearance occurred. This was left to stir overnight. The yellow solution was then evaporated using a Rotovap and 2.4225g yellow amic acid powder was recovered. The powder was then

added to a petri dish and placed into a 200°C oven for 2 hours, then 230°C for 30 minutes to yield an orange imide powder.

POSS dinadic (3g batch)

In a dry N2-environment glove box, 2 solutions were made: 2.4611g POSS dianiline with 25mL THF and 0.6047 5-norbornene-23-dicarboxylic anhydride (nadic) with 6mL THF. While stirring, the nadic solution was added to the POSS solution with no change in color (clear). The solution was left to stir overnight. The solution was then evaporated using a Rotovap and 2.4903g white amic acid powder was recovered.

The powder was then added to a petri dish and placed into a 200°C oven for 2 hours, then 230°C for 30 minutes to yield an orange imide powder.

3.2.1 Characterization of poly (amic acid) molecular structure

All 1H and 13C NMR spectra were obtained from a Bruker 300 FT-NMR 300MHz. DMSO-d6 was used as the solvent.

H^1 NMR spectra were obtained of each sample after the amic acid was removed from the synthesis solvent. Figure 8 shows the theoretical structure of each sample synthesized. The colored arrows show the locations of the protons which would appear in a given ppm range. The expected and experimental results are given in tables 5 and 6 where the ppm range has been color coded to match the arrows.

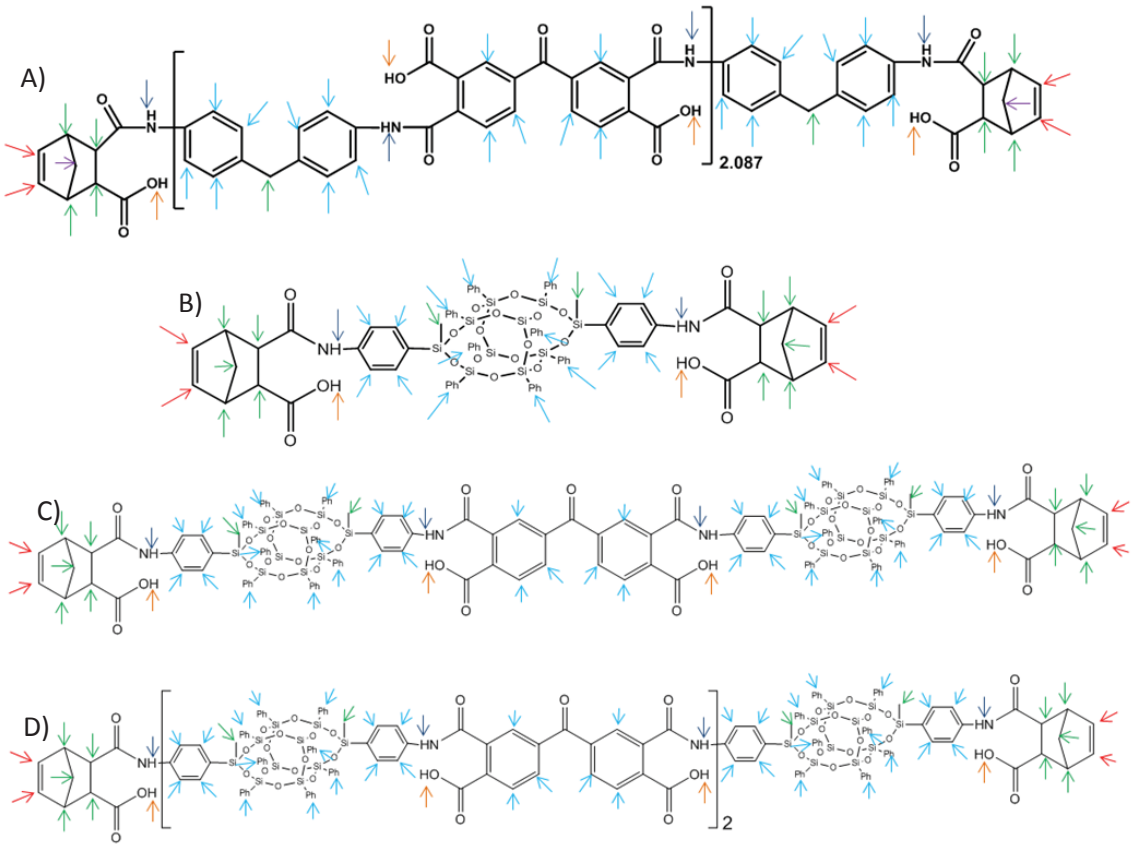

Figure 8. Proposed sample structures and proton locations for (a) PMR-15, b)POSS dinadic, c)PMR/POSS n=1, d) PMR/POSS n=2.

The data shows that the experimental data matches the expected integral values in the shown regions with the exception of the carboxylic acid and amine hydrogens. This is most likely due to these protons exchanging with the solvent and appearing at other locations in the spectra. Also not shown are methoxy groups that would form in these locations during esterification of the anhydrides.

The integrals in the 5.9-6.3ppm region, which correspond to the pair of protons on the double bond of the nadic anhydride endcap, were calibrated to 4. This was done to ascertain an average molecular weight as each molecule is theoretically capped off by two nadic monomers. The other aliphatic type protons appear in the 2.9-3.4 and 3.7-4.0ppm range. In this

region, the protons of the methylene bridge of MDA in PMR-15 also appear, as do the methyl groups on the d-silicons from the POSS dinadic. The data shows that the theoretical values of this region closely match the actual values. This gives confidence in the method of determining molecular make-up. The integrals in the 0-1.6 and 3.0-3.5 regions related to aliphatic hydrogens which appear in the nadic anhydride, POSS diamine, and MDA (for PMR—15). The 7.0-8.0 ppm region corresponds to aromatic protons in the amines, anhydrides and POSS. Again, theoretical values closely match measured ones.

Table 5. Integral values of NMR spectra peaks for PMR-15.

Integrated Range	PMR-15	
	Expected	Measured
1.25 ppm	4	4.96
6.0-6.25 ppm	37.22	58.33
7.0-8.0 ppm	4	4
2.9-3.4; 3.7-4.0 ppm	14.17	15.92
9.8 ppm	6.17	1.43
10.5 ppm	6.17	0.12

Table 6. Integral values of NMR spectra peaks for POSS containing imides.

Integrated Range	POSS dinadic		PMR/POSS n=1		PMR/POSS n=2	
	Expected	Measured	Expected	Measured	Expected	Measured
5.9-6.3 ppm	4	4	4	4	4	4
7.0-8.0 ppm	48	48.45	102	108.63	156	169.14
0-1.6; 3.0-3.5 ppm	18	17.92	24	28.8	30	35.65
10 ppm	2	1.51	2	0.64	6	0.71
11.75 ppm	2	1.97	2	1.82	6	3.76

3.3 Sample fabrication

3.3.1 Neat Resin Disc Curing

To fabricate a cured disk, a cylindrical compression mold with a 0.5 inch diameter mold cavity was charged with approximately 0.4g of imide powder. In the case of the POSS dianiline containing oligomers, a b-staging step was taken prior to molding and is discussed further in Chapter 4. A piston was inserted into the mold cavity and the mold assembly was placed into a 1-ton heated press to cure. With minimal pressure applied (just enough to contact both surfaces of the mold assembly to allow heating from the top and bottom), the temperature was ramped from RT to 536°F at 10 °F/min. A pressure of 184 psi was applied while the temperature was ramped to 599 °F at 1 °F/min. The temperature and pressure was held for 90 minutes and finally the mold was cooled to RT. A solid, dark brown colored disc was recovered and characterized.

3.3.2 Composite Panel Fabrication

One 2x2" and three 1x5" composite panels were fabricated using carbon fiber fabric and PMR-15 and POSS dinadic as the resin system.

For the PMR-15 panels, a 60 wt% solution of PMR-15 amic acid in methanol was painted onto 14 plies of carbon fiber fabric. The plies were then placed into a 55°C oven for 20 minutes to dry. The plies were then laid up in a compression mold with a perforated Teflon sheet, fiberglass fabric and a non-perforated Teflon sheet above and below the plies (from the carbon side outward). The molds were then placed in the 1-ton press and the same cure cycle as with the neat resin disc was followed.

For the POSS dinadic panels, dried amic acid powder was placed in between 14 plies of carbon fiber fabric, which was laid up similarly as with the PMR-15 panels. The molds were placed in the 1-ton press and heated from RT to 536°F at 5°F/min with 20 psi applied. The temperature was then ramped to 630°F at 2°F/minute while 187 psi was applied. This temperature and pressure was then held for 3 hours before the mold was cooled to RT.

3.4 Characterization

3.4.1 DSC

DSC experiments were carried out on a TA Instruments Q200 DSC. T-Zero DSC pans were loaded with 10-20 mg of imide powder. The experiments were performed under a nitrogen environment at a purge rate of 50mL/min. An initial ramp of 10 °C/min to 250 °C from RT was implemented to eliminate any residual solvent or water and to allow the powder to flow to form good contact with the bottom of the pan. The samples were then equilibrated at 40 °C and ramped again at 10 °/min to 315 °C. The material was then held at this temperature for 2 hours to promote curing and subsequently equilibrated at 40 °C. The final temperature ramp was done at 10 °/min to 400°C.

3.4.2 TGA

TGA experiments were performed on a TA Instruments Q5000 TGA. Experiments were conducted under both air and nitrogen atmospheres. Temperature ramps were implemented between 25°C and 900°C (some experiments only went to 600°C) at a rate of 1 °C/min and 10 °C/min.

Three temperatures of interest are shown in charts. The 5% loss temperature is the temperature at which the mass loss from the beginning of the experiment is 5%. The cure finish temperature is an estimate of when the curing process was finished. Some of the data

show a clear step after cure and before decomposition. The point at which this step flattened was taken as this temperature. When a clear step was not shown, the inflection point between cure completion and decomposition was determined. Finally, the 5% loss post-cure temperature was the temperature at which the mass loss from the mass at the cure finish temperature was 5%.

3.4.3 Density Measurements

Density measurements were performed using a Mettler-Toledo Density Kit for an MS-S Analytical Balance. The sample is first weighed in air and then in a liquid, usually water or ethanol. The mass difference, governed by Archimedes' principle, is used to calculate density. The liquid used was ethanol. Three measurements were taken and the average is presented.

3.4.4 TMA

TMA experiments were conducted using a TA Instruments Q400 TMA. A quartz expansion-type probe was used and the furnace was purged with a nitrogen atmosphere. The TMA mode was set to dynamic mode in order to modulate the force to elucidate storage and loss modulus data. A 12.5 mm diameter disc approximately 2 mm thick was placed on top of a quartz stage in the sample chamber. The expansion probe was then brought into contact with the sample to measure an initial thickness. Then a compression force of 0.2000 N was implemented by the probe and the temperature was equilibrated at 100°C. Force was modulated at 0.05Hz at an amplitude of 0.10N. The temperature was then cycled between 200°C and 100°C for two iterations. The temperature was then ramped at 5 °C/min to 360-400°C, cooled at 5 °C/min to 100 °C, and again ramped at 5 °C/min to 360-400°C. The cured glass transition temperature was ascertained from the last temperature ramp.

3.4.5 Moisture Uptake

A 2L Erlenmeyer flask was filled with approximately 1750mL of de-ionized water and heated until boiling. Specimen discs were thoroughly dried in a vacuum oven for 3 days or until weight stabilization occurred. All specimens were weighed and then placed into the flask. At approximately 1 hour intervals, the samples were removed from the boiling water, blotted dry with paper media, blown dry with nitrogen, and weighed. The samples were then placed back into the boiling water and the process was repeated until the eighth interval at which time the samples were left overnight in boiling water before the final weight measurement.

3.4.6 Long-Term thermal oxidative stability (TOS)

Long-term isothermal TOS experiments were conducted in a Lindeberg Blue M tube furnace, at 316°C. An air-generator fitted with a flow meter was connected to the tube such that a continuous flow of 100ml/min of air flowed across the samples. The cured discs were placed onto a graphite boat which was wrapped in either an aluminum or copper mesh to provide support to the discs and to facilitate gas flow above and below the samples. Disk mass measurements were taken at 3-4 day intervals. Figure 5 shows the tube furnace and samples atop aluminum mesh on the graphite boat.

3.4.7 Rheology

Rheological experiments were carried out on a TA Instruments Discover DHR3 rheometer. The samples were loaded onto 25mm stainless steel parallel plates with a gap of 0.750mm. During the oscillatory experiments, the strain amplitude was set to 1% and angular frequency was ramped from 0.1 to 100 rad/s. All experiments were carried out at 250°C.

3.4.8 Acid Digestion

ASTM D3171 was followed to determine fiber, resin and void content of the carbon fiber composite panels. Procedure B was followed with sulfuric acid as the digesting solvent with hydrogen peroxide.

3.4.9 Flexural Strength

A four-point bend test was performed in accordance with ASTM D7264. The 3 1x5 in. composite panels of each resin type were machined into the appropriate geometries, allowing for one test coupon per panel. The thickness of each panel was approximately 0.1 in.

3.4.10 Short Beam Shear Strength

A three-point bend test was performed in accordance with ASTM DD2344. The 2x2" composite panels of each resin type were machined into the appropriate geometries, allowing for multiple test coupons per panel. Five coupons were machined and tested. The thickness of each panel was approximately 0.1 in.

Chapter 4: Rheology of Uncured Resins and Curing Rheology

4.1 Resin Transfer Molding

Resin transfer molding (RTM) has become an increasingly common form of manufacturing composite parts. Industry prefers this method over compression molding or autoclave curing because RTM:

- Allows for more complex geometries
- Requires lower pressures during cure
- Has reduced capital costs
- Causes less waste
- Reduces air entrapment in the part
- Produces good surface quality
- Lowers environmental impact

RTM is a method of compression molding composites where the resin system is injected directly into a mold containing the reinforcement fibers. The part is then heated under pressure to cure the resin, producing the final part geometry. For long continuous fiber composite parts, thermoplastic resins are typically polymerized in-situ due to high viscosity of most molten resins. The monomer systems are injected into the mold and polymerized after. Thermosetting polymer resin systems offer other unique challenges due to the increase in viscosity during cure.

RTM does have limitations. In order for a resin to be qualified for RTM, it must be able to be injected and flow through the reinforcement to fill each cavity of the mold. For this, a minimum viscosity must be achieved which depends on reinforcement type and mold geometry. Thermoplastics can be heated to reduce viscosity up to the point at which

degradation becomes a concern. However, curing kinetics must be taken into consideration when heating thermosets.

4.2 Viscosity

It has been shown that inclusion of POSS dianiline into the backbone of polyimides reduces the viscosity of the uncured oligomers (Pinson 2013). This was a positive result due to improved processability of the oligomers. Similar rheological experiments were carried out on the present materials.

Table 7. Molecular weights of oligoimide samples.

Sample	**PMR-15**	**PMR/POSS n=1**	**PMR/POSS n=2**	**POSS dinadic**
Molecular Weight (g/mol)	1,005.99	3,250.45	4,872.63	1,628.27

Figure 9 shows the results of the oscillatory rheological experiments as dependence of complex viscosity on frequency at 250 °C. Although PMR-15 has the lowest molecular weight (table 7) in the oligoimide state, it still has a viscosity several orders of magnitude higher than the POSS containing oligoimides. Taking the viscosity at 0.1 $\frac{rad}{s}$ as an extrapolation to zero-shear viscosity, PMR-15 has complex viscosity of 1.01×10^6 cP, PMR/POSS n=2 at 4.98×10^5 cP, PMR/POSS n=1 at 1.05×10^5 cP and POSS dinadic at 1.39×10^4 cP. It has proposed that the reduction in viscosity is due to the size of the POSS cage interfering with oligomer chain packing and charge transfer complex (CTC) interactions (Pinson).

CTC interactions involve intramolecular or intermolecular charge transfer interactions between electron-donating diamine groups and electron-accepting dianhydride groups (Kotov

1977). Many of the mechanical, optical and electronic properties of aromatic polyimides are due to these complexes. (Hasegawa 2001). The pale yellow to deep brown color of most polyimides has also been attributed to these interactions (Ando 1997). The steric hindrance imposed by the comparatively large POSS cages interrupt these interactions resulting in reduced viscosities.

The POSS containing materials showed that viscosity has a dependence on molecular weight. POSS dinadic, with the lowest molecular weight, shows the lowest complex viscosity and a strong dependency of complex viscosity on frequency. PMR/POSS n=2, with the highest molecular weight, shows the highest complex viscosity of the POSS containing materials.

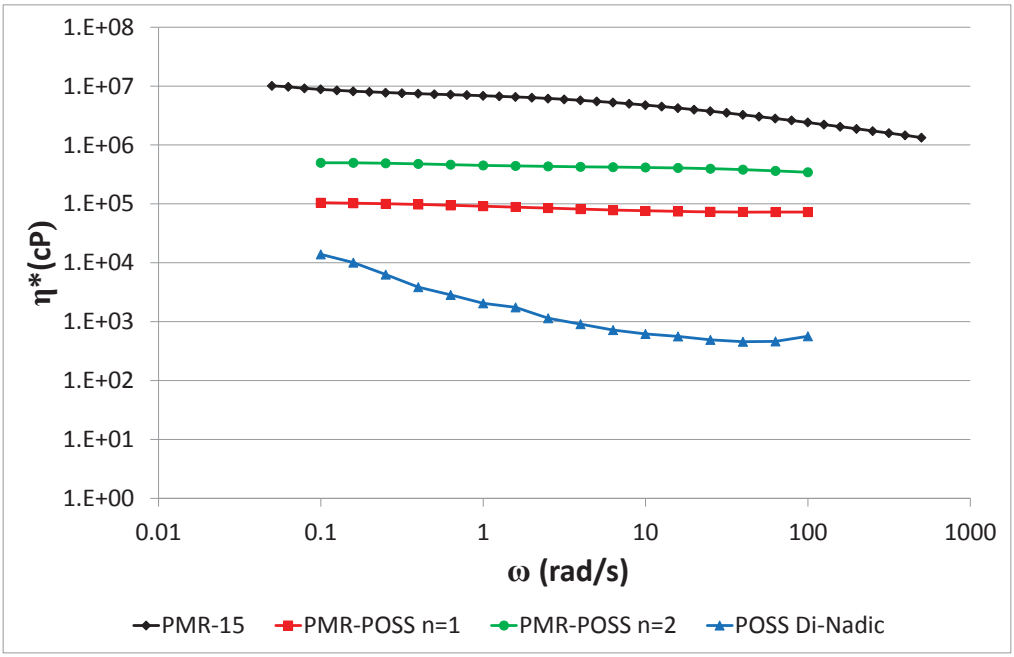

Figure 9. Complex viscosity of pre-cured oligomers as a function of angular frequency at 250 °C.

The reduction in viscosity has a direct impact on processability. Lower viscosity materials require less force to flow at a given temperature, therefore less stress on manufacturing equipment. However, for a resin to be used in an RTM process, its viscosity must be low enough to flow through the mold and completely wet the fibers. Degree of wet-

out on the fibers is subject to several processing parameters, including resin viscosity (Hedley 1994). The lower the viscosity, the easier it is for the resin to flow and saturate the fibers.

Viscosity ranges of 100-1,000 cP are typically desirable for RTM (Campbell 2003). However, this is not a well-defined range as it has been found empirically. Campbell refers to Darcy's law of flow which is followed by resin injection. Equation 1 below shows the relationship between flow rate per unit area (Q/A), reinforcement permeability (k) pressure gradient (ΔP), viscosity (η) and flow length (L):

$$\frac{Q}{A} = \frac{k*\Delta P}{\eta*L} \tag{1}$$

From this equation, it is easily seen that lower viscosity leads to higher flow rate of the resin through the reinforcement. There are multiple variables involved, such as part geometry and permeability of the reinforcement, so the maximum viscosity for proper resin flow is different for different systems.

For a RTM process to be deemed viable for a particular resin/fiber system, a good quality part must be fabricated. This means that the resin completely wets out the fibers. The resin must completely flow through and coat all of the reinforcement material. There must also be a minimum amount of voids in the matrix. Void volume can be up to 5 vol% in some cases and still be considered a quality part.

Several studies have shown that higher viscosity resins can be amenable to curing via this method, resulting in good quality parts. Adams et al. studied forced in-plane flow of an epoxy with a viscosity of 9,400 cP in an RTM-type process (Adams 1986). In a similar process, the same group studied an epoxy with viscosity of up to 20,000 cP at 22.5 °C (Adams 1987). Kiuna et al. developed curing kinetics models for epoxy resins in the range of 200-1400 cP which are used in RTM processes (Kiuna 2002).

The rheological study shows that POSS dinadic is a viable candidate for RTM. With a complex viscosity of 1.39x10^4 cP at 0.1 $\frac{rad}{s}$ and 250 °C, it easily falls into a range which has been shown to be amenable to RTM. Also, the layup procedure employed to cure the composite panel with POSS dinadic mimicked a RTM process. Due to the resin not being applied to each fabric ply and only in the center of the part, the resin had to flow through the fabric in order to completely wet the fabric and fill out the part. This was done successfully through heat and pressure similar to RTM.

4.3 Cure Rheology

Due to reduced viscosity of the POSS containing oligomers, compression mold curing proved to be a difficult process. As the material heated and its viscosity lowered, the applied pressure forced most or all of the material to bleed out of the mold. Figure 10 below shows the compression mold with bleed out through the top of the cylinder of POSS dinadic during a standard cure for PMR-15.

Figure 10. Disc fabrication compression mold with POSS dinadic material bleed out.

A b-staging method, in which the oligomers were partially cured to increase viscosity prior to compression molding, was implemented to increase the baseline viscosity during cure to prevent bleed out. The b-staging process is described below.

Figure 11(a) shows the complex viscosity of the control material during the cure process. The data is unreliable prior to reaching approximately 225 °C due to the temperature being below the material's T_g. Uncured T_g values of each sample as determined by DSC measurements during the initial heating ramp are shown in table 8. The values are only reported here and will be discussed further in chapter 5. Once the temperature rises above 225 °C, the material is able to flow and make good contact with the platens. With increasing temperature, the viscosity decreases as expected until approximately 275 °C where it begins to rise as curing begins. From 275 °C to 330 °C there are competing effects between increase in temperature which decreases viscosity, and curing which increases viscosity. After going through a local maximum viscosity at 285 °C, viscosity decreases until 330 °C where the curing process takes over and viscosity rises through the completion of cure. The strategy of b-staging was to partially cure the POSS containing oligomers until its viscosity reached the minimum viscosity of the control during the cure cycle, at approximately 295 Pa·s. A plot of POSS diPEPA during b-staging is shown in figure 11(b). The temperature profile of the b-staging process was noted and implemented during compression molding of neat resin discs.

Table 8. Uncured T_g values as determined from DSC measurements.

Sample	**PMR-15**	**PMR/POSS n=1**	**PMR/POSS n=2**	**POSS dinadic**
Uncured T_g (°C)	200.3	159.3	170.7	115.6

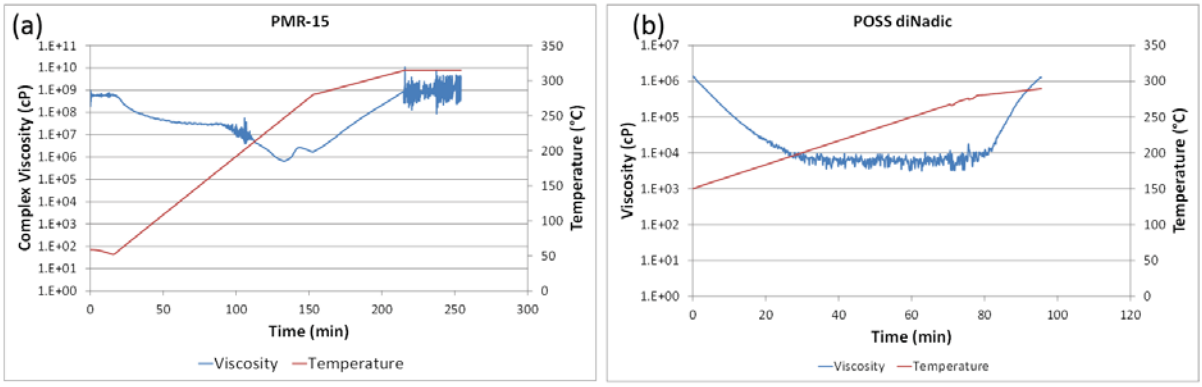

Figure 11. Complex viscosity of (a) PMR-15 through the cure cycle and of (b) POSS dinadic through the b-staging process.

Chapter 5: Properties of Uncured Neat Resins, Cured Neat Resins and Composites

5.1 Moisture Uptake

Figure 12 shows the amount of water mass that cured neat resin samples absorb over time while suspended in boiling water. PMR-15 shows a steadily increasing moisture uptake for the first eight hours. However, the rate at which moisture is absorbed decreases with time. After 24 hours, the sample is fully saturated. A measurement was taken at 48 hours (not shown) which confirmed this. Within the first two hours, each of the POSS containing materials becomes fully saturated.

The initial mass of the samples was between 0.2 and 0.4 g, therefore a difference of 100 μg can result in a percent change of 0.05%. Due to this, the change in mass over this range of time after the first two hours is taken to be negligible and the samples are assumed to be fully saturated. Slight increases and decreases in mass gain after that time are likely due to different amounts of residual water adhering to the surface of the samples while measuring mass during the experiment.

The total amount of moisture absorbed as a percent of initial mass is given in table 9. The control sample absorbs approximately 4.5% of its initial mass, while each of the POSS containing materials absorb around 1%.

Table 9. Total moisture mass gain of fully saturated materials.

Material	**Saturated Mass Gain**
PMR-15	4.5%
PMR/POSS n=1	1.1%
PMR/POSS n=2	0.93%
POSS dinadic	1.2%

Pinson et al. also studied moisture uptake in POSS containing polyimides by incorporating POSS into the backbone of polyimides that were end capped by phenylethynyl phthalic anhydride (PEPA). In their study, the moisture uptake was done in a humidity chamber at 80 °C and 80% relative humidity, therefore the moisture ingress was slower. They were able to see that the kinetics of moisture uptake was higher in the POSS containing samples due to higher amounts of free volume caused by lower cross-link density providing a greater ability for the water molecules to flux into the system. This can also be seen in the present study as the POSS containing samples were fully saturated within the first two hours and PMR-15 took over eight hours to become fully saturated.

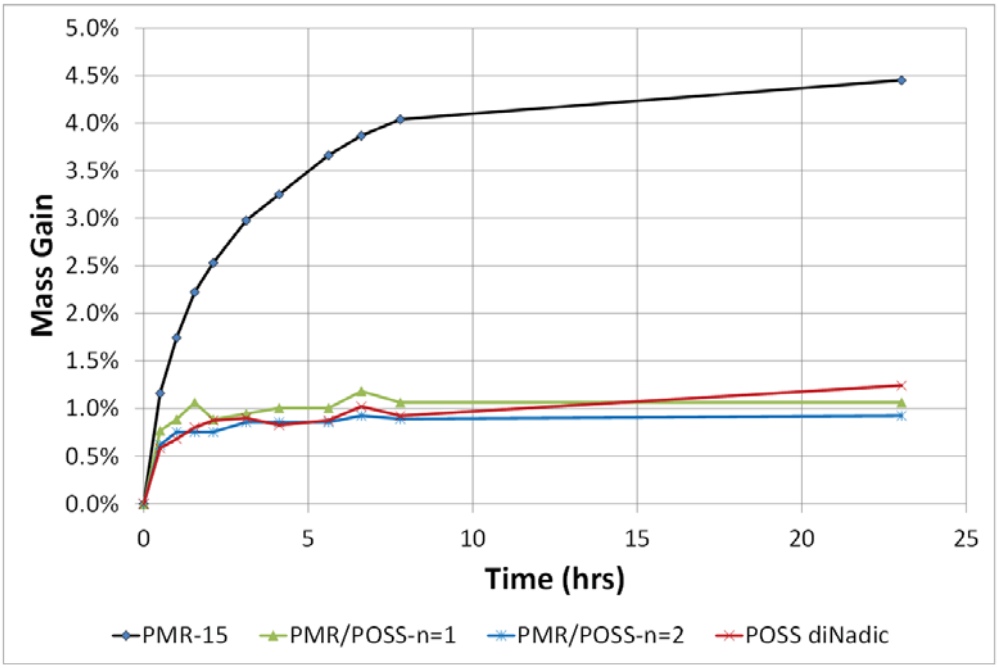

Figure 12. Moisture uptake of cured neat resin samples in boiling water as a function of time.

While the water flux was higher in the POSS containing samples, they noted also that the total moisture uptake was much higher in the control sample than in the POSS containing ones. It was postulated that this was due to fewer sites being available for water molecule

occupation. The cause of this was due to the POSS cages shielding the imide carbonyl groups from hydrogen bonding with water, similar to the disruption of the CTC interactions.

Although this has not been proven, it is known that POSS imparts hydrophobic character to materials they are either mixed with as an additive or in polymers that have POSS cages covalently bound (Parameswara 2011, Tan 2011, Pan 2015, Watanabe 2013). More specifically, it was reported that a POSS modified Kapton-like thermoplastic material exhibited approximately 80% less moisture uptake than did the material without POSS (Wu 2007). Therefore, it is hypothesized that incorporation of the POSS cages into the backbone of these PMR-15-type polyimides reduces the total moisture sorption due to its hydrophobic character.

The moisture uptake data for PMR-15 has been plotted against the square root of time and was normalized to thickness in figure 13 (symbols). Also plotted are the results of data fitting using a Fickian diffusion model (solid line). The model used to plot the fitting curve is given in equation 2 (Bhargava 2006), where M(t) is sample mass at time t, M_0 is the initial sample mass, M_∞ is the saturated sample mass, D is the diffusion coefficient and h is the sample thickness.

$$G(t) = \frac{M(t)-M_0}{M_\infty - M_0} = 1 - \frac{8}{\pi^2}\sum_{m=0}^{6} \frac{1}{(2m+1)^2} exp\left[\frac{-D(2m+1)^2\pi^2 t}{h^2}\right] \quad (2)$$

The diffusion coefficient for water ingress into PMR-15 in boiling water was calculated to be 2.1×10^{-5} $\frac{mm^2}{sec}$ by applying a least-squares minimization of equation 2. The curve representing this model has a value of 0.034 at t=0 due to the truncation of equation 2 to 6 terms, the actual value should be 0. This result is similar to that found by Pinson et al. for the phenylethynyl end capped polyimide without POSS incorporation (2.3×10^{-5} $\frac{mm^2}{sec}$). For the

POSS containing samples, the diffusion occurred too quickly and an insufficient number of data points at early times prevented a similar evaluation of diffusion coefficients.

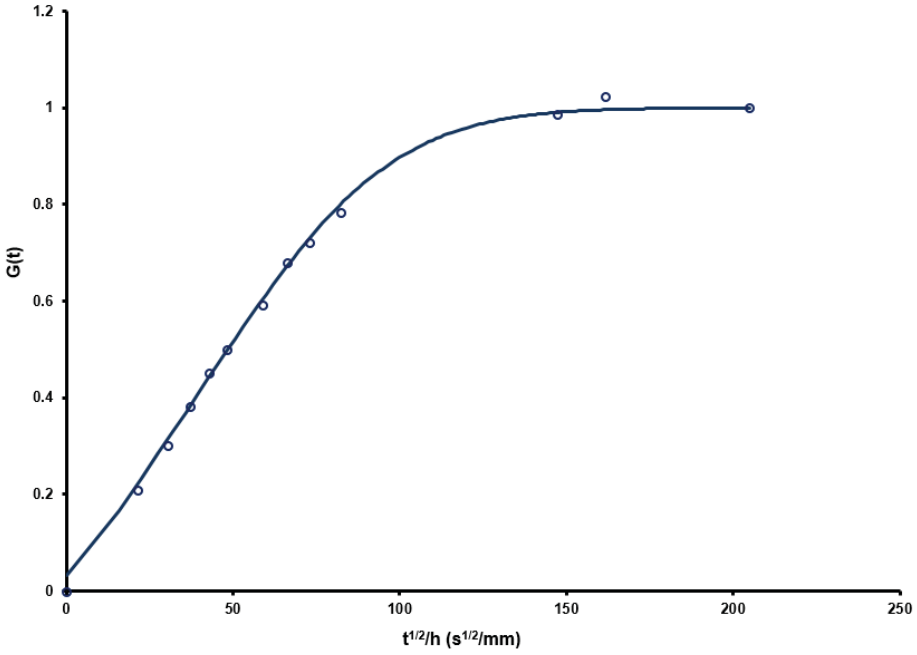

Figure 13. Normalized water absorption data of PMR-15 (symbols) and line fitting using Fickian diffusion model.

5.2 Thermal Analysis

5.2.1 Glass Transition Temperature (T_g)

5.2.1.1 Differential Scanning Calorimetry (DSC)

DSC measurements show that PMR-15 has an uncured T_g at 200.3 °C and the fully cured material has a T_g at 341.2 °C. These values are similar to what has been reported in literature (Scola 1988). When POSS is substituted for MDA in the backbone, a significant reduction in T_g occurs in both the cured and uncured state. These values are shown in table 10 and representative DSC scans are shown in figure 14. The values are taken as the midpoint of the inflection during the transition. The curve for cured PMR-15 is ambiguous as to whether it is a T_g or degradation. Immediately following the T_g is a steep exotherm representing degradation. This same exotherm is evident in the POSS dinadic curve and the PMR/POSS

n=1 and n=2 curves also trend upward, but are separated from the T_g more than with PMR-15. This occurs at approximately the same temperature as where obvious degradation occurs, as is seen in the TGA data of figure 18. However, in the next section, the T_g value is confirmed by TMA measurements and is corroborated by findings in the literature.

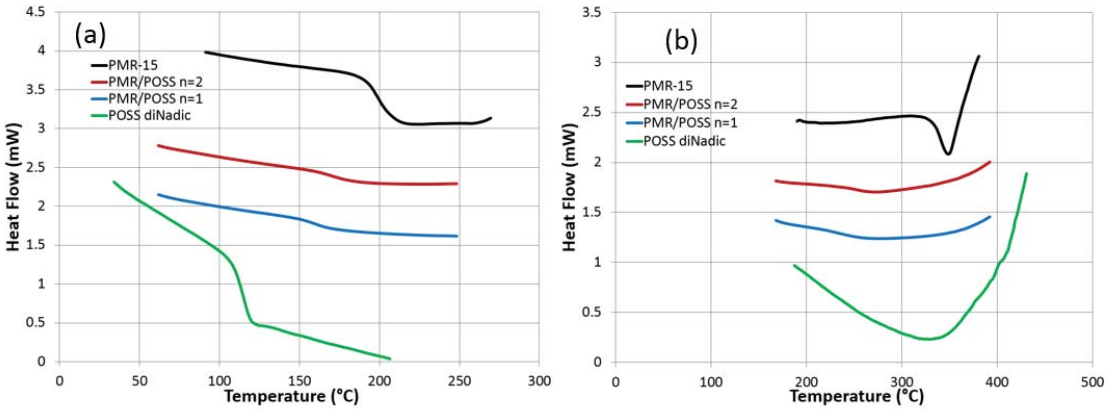

Figure 14. Representative DSC scans of (a) uncured oligomers during first heating ramp and (b) cured samples during second heating ramp.

While a reduction in T_g for the oligomers compared to PMR-15 in the uncured state is a positive because it reduces the temperature needed for the material to flow, the reduction in the cured state is a negative because it reduces the operational temperature of the resin. Both PMR/POSS n=1 and PMR/POSS n=2 fail to meet the goal of having a T_g within 5% of the control material. The cured T_g of POSS dinadic was unable to be determined by DSC. This is presumably due to the network being too constrained due to the high cross-link density to reveal the transition by this method.

Table 10. Glass transition temperatures as determined by DSC experiments.

Material	T_g (°C)	
	Uncured	Cured
PMR-15	200.3	341.2
PMR/POSS n=1	159.3	229.8
PMR/POSS n=2	170.7	252.5
POSS dinadic	115.6	-

Figure 15 shows that the uncured and cured T_g can be manipulated by blending PMR/POSS n=1 and PMR/POSS n=2 with POSS dinadic. Blends with 25, 50 and 75 wt% POSS dinadic were made and the T_gs were nearly linearly dependent on the amount of POSS dinadic added. These T_g values were also taken from DSC measurements for consistency. The DSC curves show a single transition for the uncured materials instead of one for each of the constituent materials which may be expected. The traces of the cured materials also show a single transition which is to be expected as the combination of oligomers form a single network.

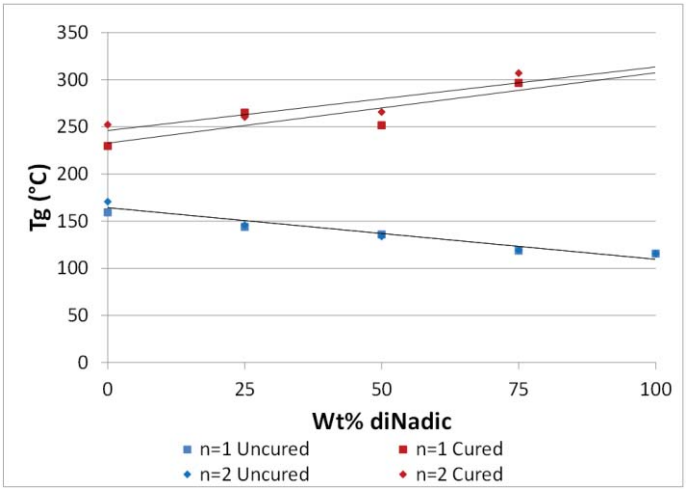

Figure 15. Glass transition temperatures of blends of PMR/POSS n=1 and PMR/POSS n=2 with POSS dinadic in the uncured and cured state via DSC measurements.

5.2.1.2 Thermomechanical Analysis (TMA)

TMA experiments show similar trends in T_g values for the samples. These values are tabulated below in table 11. TMA experiments can give different values for the T_g based on how it is calculated. Typically, the lowest value is given by the inflection point at the change in slope of the dimension change curve. Next highest is the drop-off in storage modulus. Second highest values are given by the peak in loss modulus, while the highest T_g is typically given by the peak in the tan delta curve. The tan delta, also known as loss factor or damping coefficient, is simply given as a ratio of loss modulus to storage modulus, thus it is a unitless quantity. Representative TMA plots are shown in figure 16.

Table 11. Glass transition temperatures as determined by various methods from TMA experiments.

Sample	T_g (°C)			
	Storage Modulus	Loss Modulus	Tan Delta	Dimension Change
PMR-15	343.04	365.9	374.17	319.37
PMR/POSS n=1	300.99	315.18	320.86	265.02
PMR/POSS n=2	287.54	303.46	311.82	273.57
POSS dinadic	304.32	315.06	325.77	292.74

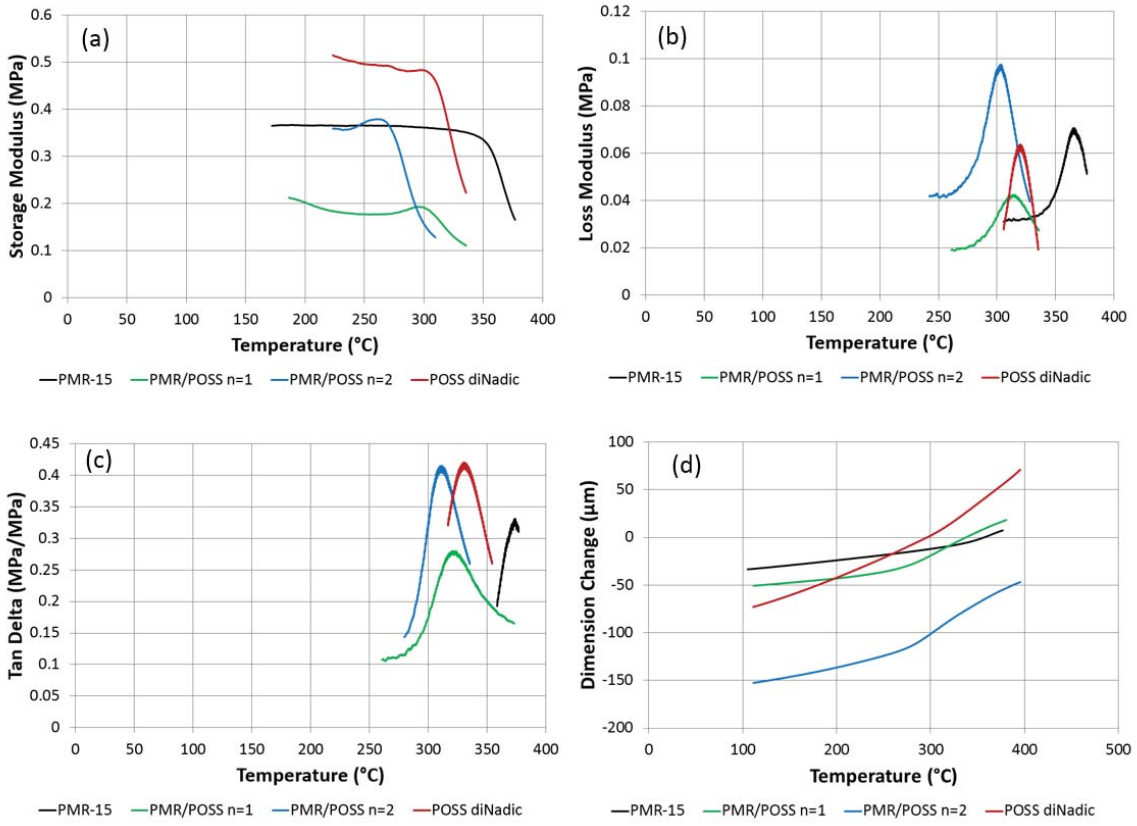

Figure 16. Representative TMA plots for each method of determining T_g including (a) storage modulus, (b) loss modulus, (c) tan delta and (d) dimension change.

Comparing the values of each sample with the same method of determining T_g does not consistently yield the same trend. However, PMR-15 has the highest cured T_g in all cases. Among the POSS containing materials, PMR/POSS n=2 shows the lowest T_g. This can be attributed to it having the lowest cross-link density among the POSS containing samples with the exception of the dimension change value where PMR/POSS n=1 has the lowest value. The T_gs of PMR/POSS n=1 and POSS dinadic are similar in all cases except for the dimension change value. Although PMR/POSS n=1 has a lower cross-link density than POSS dinadic, it also has a lower POSS concentration. These two factors are essentially canceled out and the T_g value is similar to POSS dinadic. As with the T_gs calculated from DSC experiments, all of

the POSS containing materials fall short of the goal of being within 5% of the control, PMR-15.

The nature of the Si-O-Si bonds in the POSS cage having increased torsional ability (Weinhold 2011) gives rise to the POSS cage conforming with bond angles ranging between 90° and 180° (Evmeneko 2011). This flexibility of the POSS cage itself is another contributing factor to reduced T_g in the POSS containing material. Also, the higher free volume associated with the POSS cage architecture can contribute to reduction of T_g. (Przadka 2015).

Due to the ambiguity of the transition occurring around 340 °C in the DSC curve for cured PMR-15 coupled with TGA data showing the onset of degradation between 350 and 400 °C (section 5.2.2.1), it is necessary to confirm the T_g with data from other studies. Numerous examples of T_g findings can be found in the literature for PMR-15. Depending on the method of calculating T_g, values of 333-348 °C have been reported for PMR-15 (Chuang 2007, Scola 1998, Chuang 2010). A report on PMR-15 composites also shows T_g values from dynamic mechanical analysis (DMA) (Bowles 1995). This method is very similar to TMA. A beam of the sample is put into a slight bending moment from a three-point bend apparatus and the force is modulated. Storage/loss moduli and tan delta values can be calculated from the data. Figure 17 below shows the DMA results from this report and the T_g of PMR-15 was found to be 341 °C at the drop-off of the storage modulus, the same method as is reported here in table 11. The samples were subjected to a post-cure thermal treatment at 316 °C for 16 hours and the samples studied here were not. However, after aging for 500 hours at 316 °C, the T_g only increased by 17 °C, therefore it is safe to assume that the T_g after curing at 316 °C for 1.5 hours (as was done in this study) is not much different than after a 16 hour post-cure. The reports from the literature help corroborate the findings in the present study that the T_g of PMR-

15 is approximately 340 °C, even though there is evidence of degradation at temperatures not much higher.

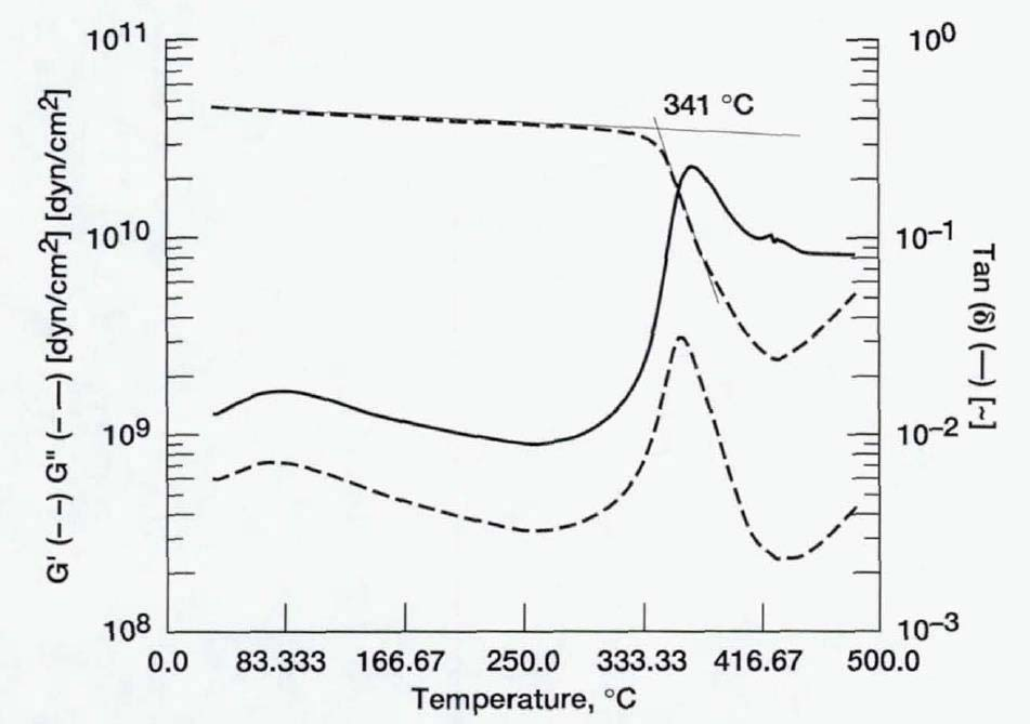

Source: Bowles, 1995

Figure 17. DMA data from experiments on PMR-15 composites showing storage/loss modulus and tan delta. The T_g from the drop off in storage modulus was found to be 341 °C.

5.2.2 Thermal Stability

5.2.2.1 Thermogravimetric Analysis (TGA)

TGA experiments were done on both PMR-15 and POSS dinadic. The machine was loaded with oligoimides and heated at 10 °C per minute to 900 °C. The initial loss in mass is due to evolution of cyclopentadiene during cure (Alston, 1992). The second mass loss event is due to degradation of the network and is the critical temperature at which the resins are no longer useful. Figure 18 below shows representative TGA curves in an oxidizing (air) environment and an inert (nitrogen) environment. In both environments, POSS dinadic was

stable to higher temperatures. Also, in both environments, POSS dinadic had a higher char yield. That is, a higher percentage of the mass remained in the sample pan as char. This is due to the silicon atoms in the POSS cage forming silica particles which are stable at extremely high temperatures. In POSS dinadic, the silicon atoms account for 17.2% of the mass and when combined with oxygen, the SiO_2 molecules that form equate to 36.9% of the initial mass which is approximately the difference in char yield between POSS dinadic and PMR-15 in an oxidizing atmosphere. In an inert atmosphere, the phenyl groups will form carbonaceous char that does not volitalize. This is the reason for the char yield to be greater than 0 in both cases. In POSS dinadic, there are more phenyl groups attached to the POSS cage and the cage itself will not volitalize during decomposition. Therefore, a higher char yield results for POSS dinadic than for PMR-15.

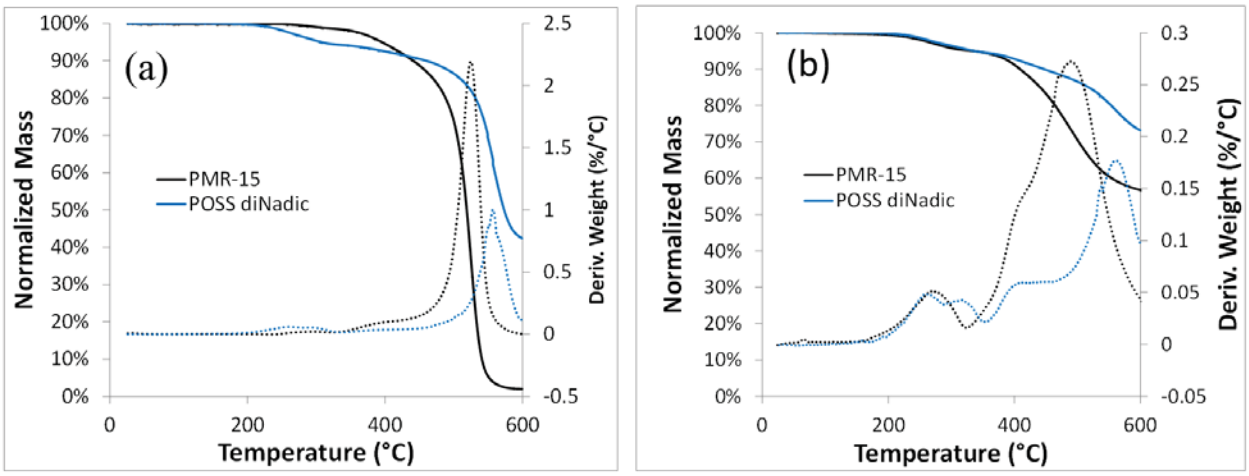

Figure 18. TGA plots of PMR-15 and POSS dinadic beginning with oligoimides in (a) oxidizing and (b) inert environment.

5.2.2.2 Resin Long Term Thermal Oxidative Stability (TOS)

The TGA results were used as a screening tool due to the ease of experimental setup and length of time the experiments take. A much better tool to determine thermo-oxidative stability is a long-term study at high temperatures near the service temperatures of the

composites. Typically for PMR type resins, specific temperatures are studied for these long-term studies. Most TOS studies include 288 °C because that is the maximum service temperature of PMR-15 (Tandon 2007). Higher temperatures, such as 316 and 343 °C have also been found in the literature as testing temperatures (Tandon, Bowles 1994, Bowles 1998, Madhukar 1997). For the present study, 288 and 316 °C were chosen.

Figure 19 shows the results of this study as neat resin discs were subjected to 316 °C while air flowed across the samples. The figure shows percent mass loss as a function of time exposed to the conditions. Contrary to the TGA results, POSS incorporation into the network has a deleterious effect on TOS. POSS with phenyl substituents like the materials used here have been shown to be stable up to 350 °C and do not show a maximum degradation rate until 466 °C. Therefore, the POSS inclusion into the backbone is not the culprit here (Fina 2006). At similar degrees of polymerization of the oligomers, PMR-15 and PMR/POSS n=2 show similar levels of degradation. At shorter oligomer chain lengths, PMR/POSS n=1 loses more mass over time. At the shortest oligomer chain length (n=0), POSS dinadic loses almost 3 times as much as the control material.

Nadic concentration has been shown to be a factor in long-term TOS. Leung et al. studied thermo-oxidative stability of three different PMR-type polyimides (Leung 1996). The same monomers were used for each material, but the oligomer molecular weight varied in each. Molecular weights of 1,500 (PMR-15), 2,400 (PMR-24) and 2,900 g/mol (PMR-29) were use in the study. They found that at 316 °C, PMR-15 lost the most mass and PMR-29 lost the least. PMR-29 which had the highest molecular weight, thus lowest end-cap (nadic) concentration performed best in the TOS study.

These findings directly correlate with the results of the TOS study shown here. At the shortest oligomer chain length, hence highest nadic concentration and cross-link density, POSS dinadic performs the poorest among the materials studied. At the second highest level of nadic concentration, PMR/POSS n=1 performs better, but is still loses approximately 50% more mass after 675 hours at the elevated temperature. At similar nadic concentrations, PMR-15 and PMR/POSS n=2 perform similarly.

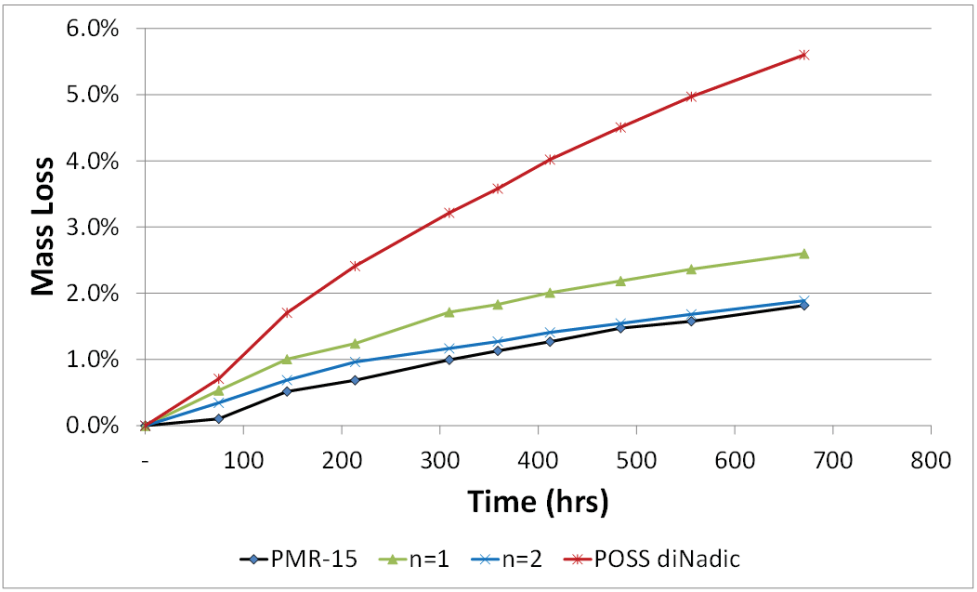

Figure 19. Mass loss over time of neat resin discs at 316 °C.

5.2.2.3 Composite Long Term Thermal Oxidative Stability (TOS)

The same TOS experiments were carried out on carbon fiber composites with PMR-15 and POSS dinadic as the matrix material. Figure 20 below shows the mass loss as a percentage of initial mass over time at 316 °C with an air flow across the samples. The total mass loss was reduced because the resin only made up approximately 30% of the mass (section 5.3.1). The total mass loss after 630 hours of the POSS dinadic sample was about 4 times as much as the

control sample. Again, the higher nadic concentration of the POSS dinadic resin contributes to lower performance.

A common side effect of thermal aging is the development of micro-cracking in the resin system. In a study done at NASA, PMR-15 composites were fabricated with carbon fibers that had been processed to receive different surface treatments to study the effect of the fiber/resin interfacial bond strength on isothermal aging (Bowles 1994). The different specimens experienced different rates of mass loss during aging and it was shown that after a few hundred hours of aging, the mechanism of degradation changed from surface area controlled to being controlled by specimen volume. The active surfaces began to include internal cracks and promotion of nucleation of internal voids that grew and multiplied. The number of and length of the cracks increased with longer aging times. These micro-cracks and voids can lead to premature mechanical failure of the composite part.

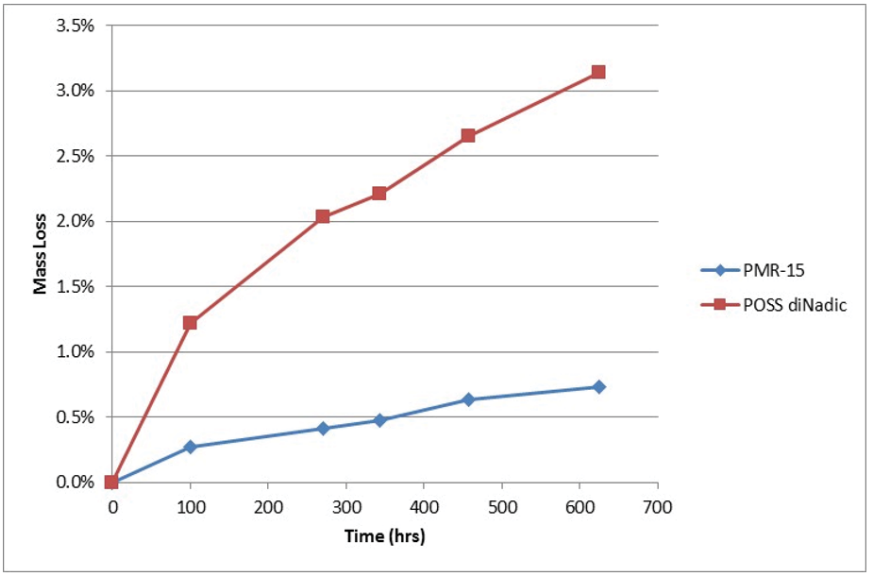

Figure 20. Mass loss over time of carbon fiber composites at 316 °C.

Figure 21 (a) and (b) show an optical microscope image of the cross section of the PMR-15 composite coupon before and after thermal aging. Prior to aging, the resin (darker color phase) shows no signs of voids or cracks. After 450 hours at 316 °C, micro-cracks begin to develop, as pointed out in the figure by the red circles. This result is comparable to the NASA study in that aging at elevated temperature induced resin cracking. Also, at longer aging times, the extent of the cracking was worse. The images at shorter times are not shown here.

For comparison, figure 21 (c) and (d) show optical microscope images at the same magnification as the POSS dinadic composite cross-section. Prior to aging, a few voids are seen in the matrix, but no cracks. After the same time aging as with the PMR-15 coupon, no micro-cracking has occurred in the POSS dinadic sample. Although the POSS containing sample performs poorly in comparison to PMR-15 in terms of mass loss, this result is a positive one.

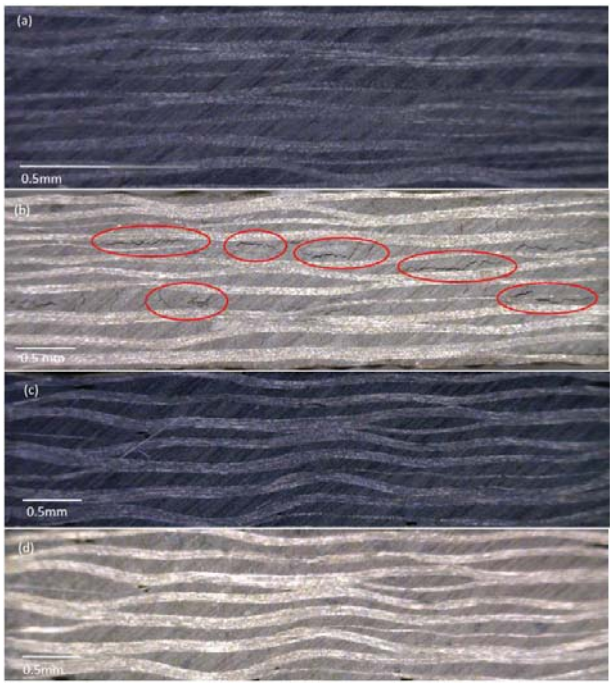

Figure 21. Optical microscope images of cross-sections of carbon fiber composites which underwent TOS treatment with (a) PMR-15 at 0 hours, (b) PMR-15 at 450 hours, (c) POSS dinadic at 0 hours and (d) POSS dinadic at 450 hours.

5.3 Composite Mechanical Properties

5.3.1 Constituent content

Due to the lay-up procedure for the PMR-15 and POSS dinadic composite panels being different, it was important to determine the constituent makeup of the final part. Mechanical properties rely heavily on the resin/fiber content of the part.

In tensile loading in the fiber direction, the strains in the fiber and resin are equal to the strain in the composite (equation 3). However, stress and Young's modulus in the composite follow a rule of mixtures (equations 4 and 5). When loaded in the direction normal to the fiber direction, the stresses in the fiber and resin are equal to the stress in the composite (equation 6). Strains in the composite follow a rule of mixtures (equation 7) and the modulus of the composite follows an inverse rule of mixtures (equation 8). In the equations below, ε_c, ε_f and ε_m are the strains in the composite, fiber and matrix, respectively; σ_c, σ_f, and σ_m are stress in the composite, fiber and matrix, respectively; V_f and V_m are volume fraction of the fiber and matrix, respectively; E_c, E_f and E_m are the moduli of the composite, fiber and matrix, respectively.

$$\varepsilon_c = \varepsilon_f = \varepsilon_m \tag{3}$$

$$\sigma_c = \sigma_f V_f + \sigma_m V_m \tag{4}$$

$$E_c = E_f V_f + E_m V_m \tag{5}$$

$$\sigma_c = \sigma_f = \sigma_m \tag{6}$$

$$\varepsilon_c = \epsilon_f V_f + \varepsilon_m V_m \tag{7}$$

$$\frac{1}{E_c} = \frac{V_f}{E_f} + \frac{V_m}{E_m} \tag{8}$$

Therefore, to directly compare mechanical properties of the different materials, the constituent content of each panel must be known. Table 12 below shows the results of the acid

digestion per ASTM D3171 to determine such values. In this procedure, three coupons weighing approximately 1 gram each are cut out of each composite panel. Density and mass are measured before they are heated in sulfuric acid until the resin is completely digested. In the case of PMR-15, this happened overnight, but for POSS dinadic the process took more than one week. Once the resin is digested, hydrogen peroxide is added and the solution becomes clear. The remaining fibers are filtered out, dried and then weighed again. These measurements, along with calculations from equations 9-13, give the constituent contents of the panel including resin weight percent, fiber volume percent and void volume percent. In these equations, M_i and M_f are the initial mass of the coupon and mass of the remaining fibers, respectively. W_m and W_f are matrix and fiber contents by mass, V_m, V_f and V_v are matrix and fiber contents by volume and ρ_m, ρ_r and ρ_c densities of the matrix, resin and composite, respectively.

$$W_m = \frac{M_i - M_f}{M_i} * 100 \tag{9}$$

$$V_m = \frac{M_i - M_f}{M_i} * \frac{\rho_c}{\rho_m} * 100 \tag{10}$$

$$W_r = \frac{M_f}{M_i} * 100 \tag{11}$$

$$V_r = \frac{M_f}{M_i} * 100 * \frac{\rho_c}{\rho_r} \tag{12}$$

$$V_v = 100 - (V_r + V_m) \tag{13}$$

Table 12. Composite constituent content of PMR-15 and POSS dinadic carbon fiber composite panels.

Resin System	Resin Content (wt%)	Fiber Content (vol%)	Void Content (vol%)
PMR-15	29.84	61.97	1.88
POSS dinadic	28.68	62.19	3.53

Both resin content and fiber content of the composite panels were nearly identical. Resin content was found to be approximately 29 wt% and the fiber content was approximately 62 vol%. The only difference was in the void content in each panel. The void content of the POSS dinadic was almost twice as high, but still well within an appropriate range for mechanical testing.

5.3.2 Flexural strength

The experimental setup as laid out by ASTM D7264 was used to determine flexural strength and modulus of both the PMR-15 and POSS dinadic composite panels. The four-point bend setup is shown in figure 22. The ratio L:H was set to 32:1 per the ASTM specifications. This flexural strength and modulus were used to compare the resins because the resin mechanical properties are much more dominant in this setup than in a typical tensile test setup where the properties are dominated by the much stronger fibers.

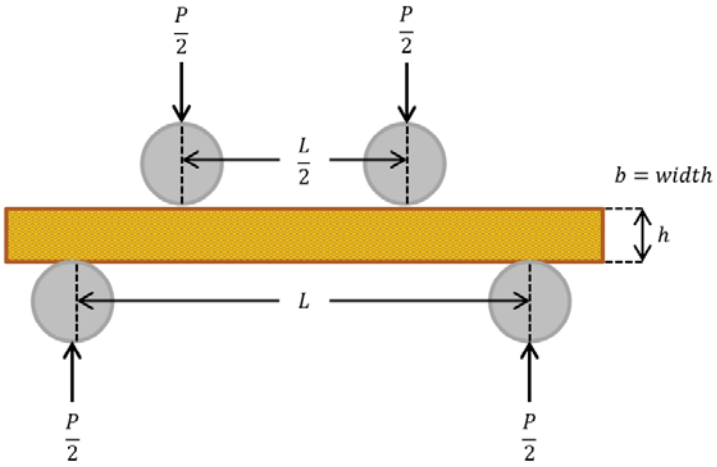

Figure 22. Experimental setup of ASTM D7264 to determine flexural strength and modulus.

Outputs of the test were given in load and displacement. To calculate stress, equation 14 was used where σ is the flexural stress, P is the load applied, L is the distance between the two bottom points as shown in the figure, b was the width of the coupon and h was the height.

$$\sigma = \frac{3PL}{2bh^2} \tag{14}$$

The ultimate fracture stress as shown in figure 23 (a) was calculated using equation 14 with the load being equal to the load at fracture. The flexural modulus, shown in figure 23 (b), was calculated as the slope of the stress-strain plot, where strain is calculated as displacement divided by initial thickness. Three samples were used for each test and the error bars shown are the standard deviations. Representative plots of the stress vs. strain curves are given in figure 24.

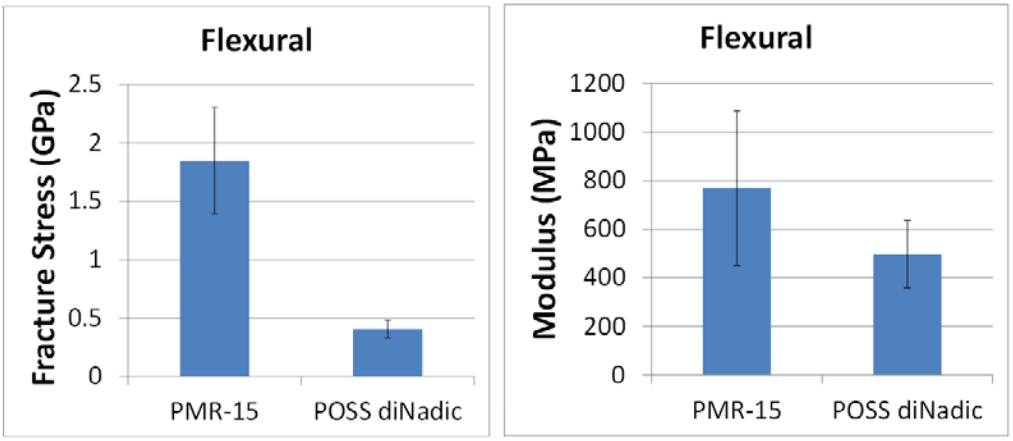

Figure 23. Flexural (a) ultimate strength and (b) modulus of PMR-15 and POSS dinadic carbon fiber composite panels.

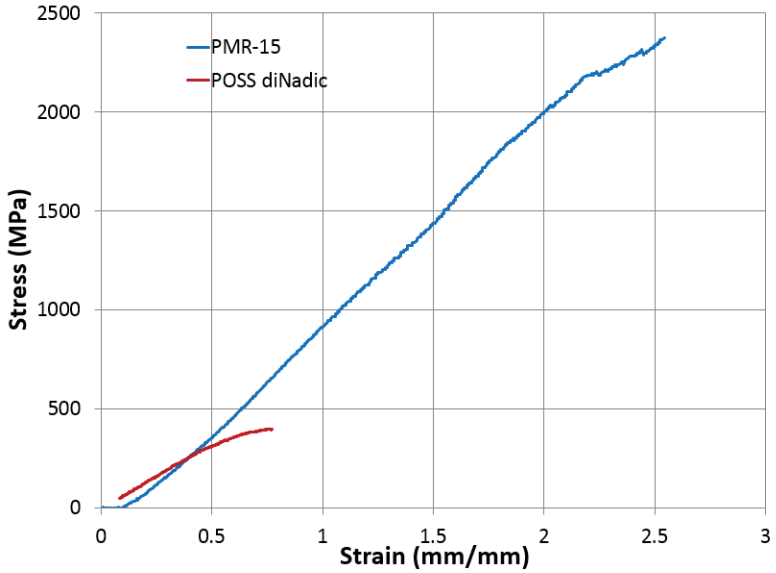

Figure 24. Representative stress vs. strain plot of the flexural strength experiments.

The flexural strength and modulus of the POSS dinadic composites were shown to be significantly lower than that of the PMR-15 composite. The ultimate strength was more than four times less than the control material. Similarly, the flexural modulus of the POSS dinadic sample is also much less than the PMR-15 sample, although to a lesser degree.

As with the previous results, the POSS cage flexibility and disruption of the CTC interactions plays a large role in properties. Here, the mechanical properties are severely depleted because of this.

5.3.3 Short beam shear strength.

The experimental setup as laid out by ASTM D2344 was used to determine short beam shear strength of both the PMR-15 and POSS dinadic composite panels. The three-point bend setup is shown in figure 25. Here the L:h ratio was 4:1 per the ASTM specifications. The increased thickness compared with the distance between the two lower points causes the stress field in the part to be much different in this experiment. Instead of simple compression and tension as with the flexural strength setup, the stresses in the center of the sample are dominated by shear. This experiment highlights the interlaminar shear strength of the resin between the fabric layers. Five samples were tested in this experiment.

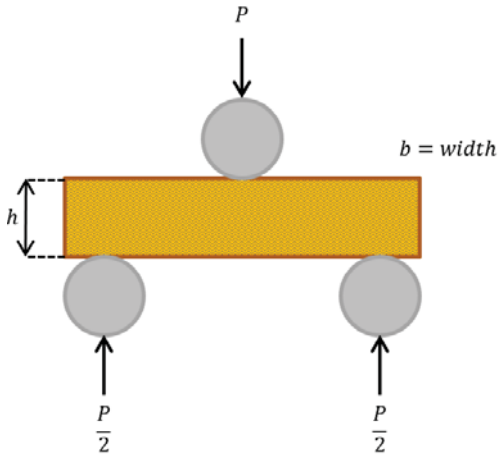

Figure 25. Experimental setup of ASTM D2344 to determine short beam shear strength.

The ultimate short beam shear strength was calculated per equation 15, where P_{max} is the load at failure, b is the width of the sample and h is the thickness.

$$F^{sbs} = Short\ Beam\ Shear\ Strength = 0.75\frac{P_{max}}{bh} \quad (15)$$

As with the flexural strength, the short beam shear strength of the POSS dinadic composite sample is much less than that of the PMR-15 sample. It is almost four times less strong than the control sample. The short beam shear strength is shown in figure 26 below, where the error bars are shown as standard deviation. Much the same as with the flexural strength, the POSS cage flexibility and disruption of the CTC interactions have deleterious effects on the short beam shear strength.

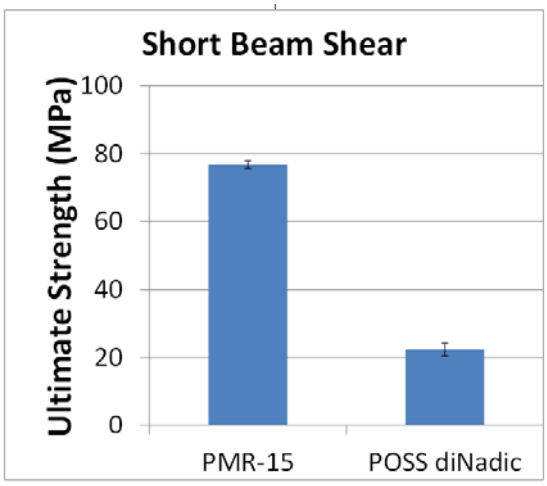

Figure 26. Short beam shear strength of PMR-15 and POSS dinadic carbon fiber composite panels.

One argument to the contrary could be the increased void volume in the experimental sample causing reduced mechanical properties. While this may be true, the slight increase in void content would not likely have an effect this large. In a study on the effect of void content on mechanical strength, Uhl et al. calculated the effect using a graphite woven mesh and epoxy matrix composite (Uhl 1988). Figure 27 shows this relationship in graphical form. The data fit shown in the figure gives a way to calculate apparent interlaminar shear strength (ISS) based on void content. In the plot, an ideal composite with zero porosity would have an ISS of 10.53 ksi. A void content of 1.88 vol% would give an ISS value of 10.39 ksi and a void content of

3.53 vol% would give an ISS value of 10.28 ksi. This is a reduction of 1.1% in ISS due to increased porosity. While this is clearly not the same system as studied in this work, the increased void content shown (1.88 vol% to 3.53 vol%) would not be sufficient enough to account entirely for the reduction in strength shown.

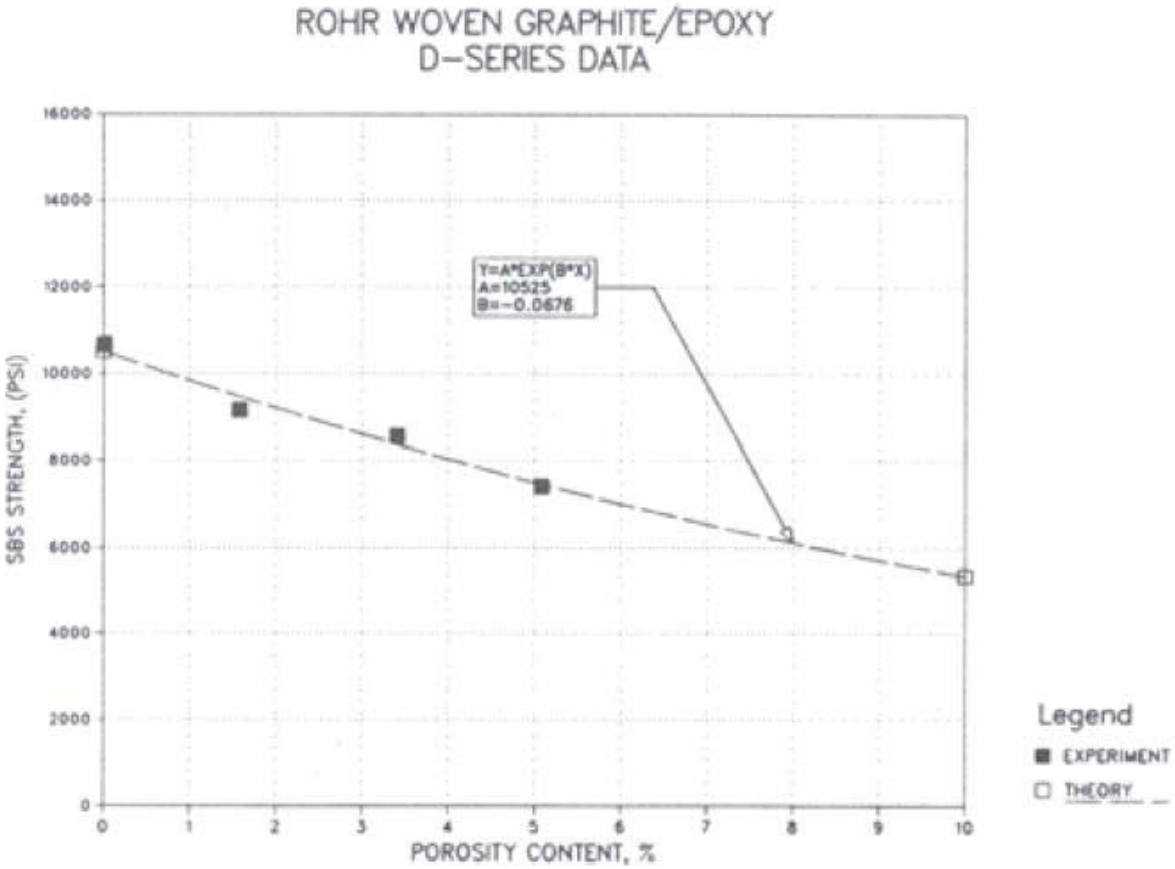

Source: Uhl 1988.

Figure 27. Short-beam shear strength versus porosity content for woven graphite epoxy laminates.

5.4 Summary

The results of resin characterization of PMR-15 and the POSS containing derivatives were similar to that shown by Pinson et al. and their work with phenylethynyl end capped polyimides. There was decreased moisture absorption of all POSS samples compared to the

control. Both DSC and TMA measurements confirmed that a significant decrease in T_g occurs when POSS is incorporated in the backbone in both the cured and uncured states. However, this can be mitigated by decreasing the oligomer chain length and increasing cross-link density. POSS dinadic achieved the highest T_g in the cured state; therefore composite characterization was only done on this material.

The thermo-oxidative stability of the materials was studied at different time scales. TGA measurements were done at relative rapid heating rates and the POSS containing samples outperformed PMR-15. However, in long term isothermal aging studies, the result was the opposite. POSS incorporation was not shown to be a factor; rather the cross-link density or concentration of nadic end caps was the culprit in the poor performing POSS dinadic. This trend continued in long term isothermal aging of POSS dinadic composites compared with PMR-15 composites. Although, the POSS sample showed no signs of micro-cracking due to thermal aging whereas PMR-15 was riddled with micro-cracks.

In mechanical testing, the properties of PMR-15 were far superior to POSS dinadic. Both flexural strength and short beam strength were significantly decreased in POSS dinadic.

Chapter 6: Conclusions

A PMR-type polyimide was synthesized with a polyhedral oligomeric silsesquioxane (POSS) dianiline as a "drop-in" replacement for MDA. Three variations with different oligomer chain lengths were synthesized and characterized. The synthesis procedures resulted in the desired chemical structures as shown by NMR. Processability was studied by characterizing the T_g of the uncured oligomers and by rheology measurements at temperatures above this T_g. Thermal stability was characterized by TGA and long-term TOS studies. Resistance to moisture ingress was studied by immersion of neat resin discs in boiling water. Values of T_g in the cured state were determined by DSC and TMA. Carbon fiber composites of PMR-15 and POSS dinadic were fabricated and characterized. Long-term TOS studies were done in the composite form and were imaged for evidence of micro-cracking. Mechanical properties were also evaluated on composite coupons.

Among the positive results were decreased moisture uptake, increased processability by a decreased uncured T_g and decreased complex viscosity, and reduced thermal micro-cracking.

The deleterious effects of POSS incorporation included reduced cured T_g in the longer chain oligomers (n=1 and n=2), reduced long-term thermo-oxidative stability in both neat resins and carbon fiber composite form, and reduced composite mechanical strength.

Chapter 7: Future Work

7.1 POSS diPEPA

Due to the TOS limitations when using POSS dinadic in the PMR-type structure, no future work is necessary with this same system. Other work has been done with POSS polyimides that use a different endcap. Figure 28 below shows the structure of POSS diPEPA, which is analogous to POSS dinadic, but has PEPA endcaps instead. This work was a follow up to the work by Pinson et al. where the oligomer chains were shortened from n=4 to n=3 in order to mitigate reduction in T_g by incorporation of POSS. The n=0 chain, POSS diPEPA, was also synthesized due to the positive results seen by POSS dinadic.

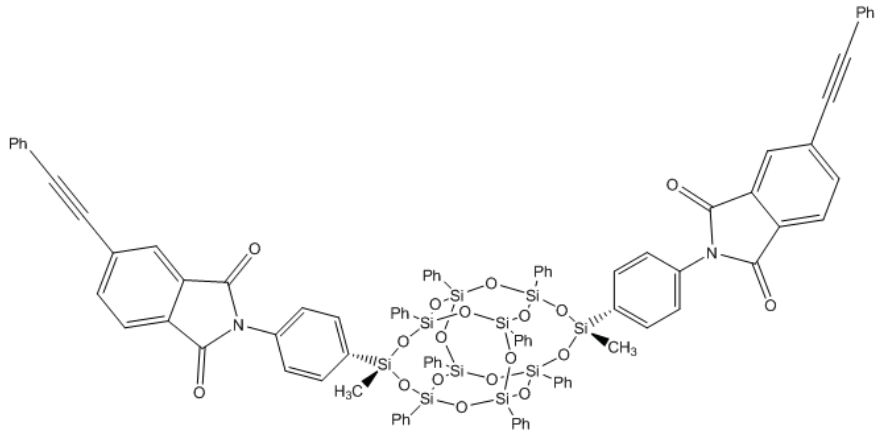

Figure 28. Chemical structure of POSS diPEPA.

All of the benefits afforded by POSS diNadic were seen with POSS diPEPA. The complex viscosity profiles are very similar, but at an order of magnitude less with POSS diPEPA. The uncured T_g as measured by DSC is 105 °C by DSC and the cured T_g was 347 °C

as measured by TMA. However, the poor TOS performance was not seen due to the lack of nadic endcaps. In the same long-term TOS study on the neat resin that was done on PMR-15, after 400 hours, the mass loss was just under 1% and for PMR-15 it was just over 1%.

In future work, it would be necessary to compare TOS and mechanical properties of carbon fiber composites containing POSS diPEPA. The same flexural and short beam shear tests would be performed using this resin system.

Although this is not a direct replacement for MDA in a PMR-type system, the results are promising for a high temperature resin system. The largest downside is the necessary curing temperature of the PEPA endcaps of 380 °C.

7.2 PMR-PCy

Another route for MDA replacement in PMR-15 that has been studied recently is that of a dianiline that is derived from a renewable aromatic compound ρ-cymene (shown in figure 29). In a separate proposal written to SERDP for the same solicitation, a collaboration between the Air Force Research Laboratory (AFRL), the Naval Air Warfare Center Weapons Division (NAWCWD), Army Research Laboratory (ARL), the Army Public Health Command (APHC) and Drexel University proposed numerous new anilines for MDA replacement. The ρ-cymene derived aniline (CDA) was developed by NAWCWD at the research laboratory located in China Lake, CA.

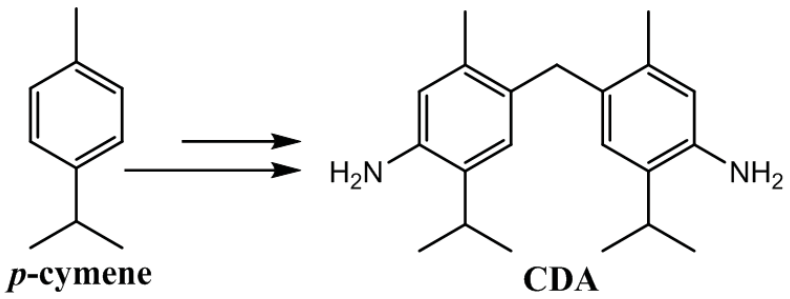

Source: Harvey 2016

Figure 29. Conversion of ρ-cymene to CDA.

The polyimide synthesized from this monomer (PMR-PCy) in the same stoichiometry as PMR-15 affords many properties that are within the 5% mark of PMR-15. The cured T_g from DSC is 323 °C and from the drop off in storage modulus in TMA is 330 °C. The complex viscosity profile is almost identical to PMR-15. The saturated moisture uptake is 1.5% less than PMR-15. Long-term TOS studies showed a slight increase in mass loss of about 1% after 350 hours. Perhaps the biggest improvement is that modeling efforts done at APHC show that CDA is non-toxic, non-mutagenic and non-carcinogenic.

Currently, efforts to fabricate carbon fiber composites with this resin system to determine mechanical properties are ongoing. Due to the similarity of CDA to MDA, it is hopeful that similar mechanical properties will be seen. Should these properties be met, further testing will ensue and real working parts will be fabricated.

REFERENCES

Adams, K.L. and Rebenfeld, L. "In-Plane Flow of Fluids in Fabrics: Structure/Flow Characterization." *Textile Research Journal* (1987): 647-654. Web.

Adams, K.L. et al. "Forced In-Plane Flow of an Epoxy Resin in Fibrous Networks." *Polymer Engineering and Science* 26. 20 (1986): 1434-1441. Web.

Alston, W.B. et al. 1992. "Cyclopentadiene Evolution During Pyrolysis-Gas Chromatography of PMR Polyimides." NASA TM-105629. AVSCOM TR-91-C-023. Print.

Ando, S. Matsuura, T. Sasaki, S. "Coloration of Aromatic Polyimides and Electronic Properties of their Source Materials." *Polymer Journal* 29. 1 (1997): 69-76. Web.

Bhargava, P. et al. "Moisture Diffusion Properties of HFBE-II-52 Polyimide." *Journal of Applied Polymer Science.* 102. (2006): 3471-3479. Print.

Bowles, K.J. et al. "Comparison of Graphite Fabric Reinforced PMR-15 and Avimid N Composites After Long-Term Isothermal Aging at Various Temperatures." *Journal of Advanced Materials.* 30. 1 (1998): 27-35. Web.

Bowles, K.J. et al. 1995. "Long Term Isothermal Aging Effects on Carbon Fabric-Reinforced PMR-15 Composites: Compression Strength." NASA TM 107129. Print.

Bowles, K.J. et al. "Thermal-Stability Relationships Between PMR-15 Resin and its Composites." *Journal of Advanced Materials.* 26. 1 (1994): 23-32. Web.

Bowles, K.J. et al. 1994. "Thermal Stability Relationships Between PMR-15 Resin and its Composites." NASA Tech Brief LEW-16202. Print.

Campbell Jr, F. *Manufacturing Processes for Advanced Composites.* Oxford, UK: Elsevier Advanced Technology, 2003.

Chuang, K. 2002. "High T_g Polyimides." NASA TM-563972. Print.

Chuang, K. 2010. "A High T_g PMR Polyimide Composite (DMBZ-15)." NASA TM. Print.

Evmeneko, G. et al. “Morphological Behavior of Thin Polyhedral Oligomeric Silsesquioxane Films at the Molecular Scale.” *Journal of Colloid and Interface Science.* 360. 2 (2011): 793-799. Web.

Fina, A. et al. “Polyhedral oligomeric silsesquioxanes (POSS) thermal degradation.” *Thermochimica Acta*. 440. 1 (2006): 36-42. Web.

Guengerich, F.P. “Cytochrome P450 and Chemical Toxicology.” *Chemical Research in Toxicology*. 21. 1 (2008): 70-83. Web.

Hasegawa, M. Horie, K. “Photophysics, photochemistry, and optical properties of polyimides.” *Progress in Polymer Science* 26. 2 (2001): 259-335. Web.

Hedley, Charles W. *Mold Filling Parameters in Resin Transfer Molding of Composites*. MS Thesis. Montana State University, 1994. Web. 2016.

http://www.denix.osd.mil/awards/upload/EEWSA-NAVAIR-NARRATIVE.pdf. Accessed May 10, 2016.

https://www.osha.gov/pls/oshaeb/owadisp.show_document?p_table=FEDERAL_REGISTER&p_id=13254 (accessed May 11, 2016).

Hughes, R.E. “Reduction of Dehydroascorbic Acid by Animal Tissues.” *Nature.* 203. 494 (1964): 1068. Web.

Kiuna, N. et al. “A model for resin viscosity during cure in the resin transfer moulding process.” *Composties Part A: Applied Science and Manufacturing* 33. 11 (2002): 1497-1503. Web.

Kopelman, H. et al. “Epping Jaundice.” *British Medical Journal.* 1. 5486 (1966): 514-516. Web.

Kotov, B.V. et al. “Aromatic Polyimides as Charge Transfer Complexes.” *Vysokomol. Soyed.* A1. 3 (1977): 614-618. Web.

Leung, C. et al. “Thermo-oxidative stability of polyimides – I. Effect of prepolymer molecular weights.” *Polymer Degradation and Stability.* 58 (1997): 11-14. Web.

Madhukar, M.S. et al. “Thermo-oxidative Stability and Fiber Surface Modification Effects on the Inplane Shear Properties of Graphite/PMR-15 Composites.” *Journal of Composite Materials.* 31. 6 (1997): 596-618. Web.

Pan, A. et al. “POSS-tethered fluorinated diblock copolymers with linear- and star-shaped topologies: synthesis, self-assembled films and hydrophobic applications.” *RSC Advances.* 5. 68 (2015): 55048-55058. Web.

Pan, G. “Polyhedral Oligomeric Silsesquioxane (POSS).” In *Physical Properties of Polymers Handbook*, ed. Mark, J.F. (New York: Springer New York, 2007), 577-584
Parameswara, R.C. and Wunder, S.L. “Polyoctahedral Silsesquioxane-Nanoparticle Electrolytes for Lithium Batteries: POSS-Lithium Salts and POSS-PEGs.” *Chemistry of Materials.* 23. 23 (2011): 5111-5121. Web.

Pater, Ruth H. Low Toxicity High Temperature PMR Polyimide. NASA, assignee. Patent US5171822. 15 Dec. 1992. Print.

Pinson, D. et al. “Thermosetting Poly(imide silsesquioxane)s Featuring Reduced Moisture Affinity and Improved Processability.” Macromolecules 46. 18 (2013): 7363-7377. Web.

"PMR-15 Polyimide Resin." Space Foundation. Accessed May 10, 2016. https://www.spacefoundation.org/programs/space-technology-hall-fame/inducted-technologies/pmr-15-polymide-resin.

"Polyimide Boosts High-Temperature Performance." Polyimide Boosts High-Temperature Performance. Accessed May 10, 2016. https://spinoff.nasa.gov/Spinoff2008/ip_5.html.

Przadka, D. “Multimethacryloxy-POSS as a crosslinker for hydrogel materials.” *European Polymer Journal* 72 (2015): 34-49. Web.

Scholz, R.W. et al. “Mechanism of Interaction of Vitamin-E and Glutathione in the Protection Against Membrane Lipid Peroxidation.” *Annals of the New York Academy of Sciences.* 570 (1989): 514-517. Web.

Scola, D.A. and Vontell, J.H. “High-Temperature Polyimides, Chemistry and Properties.” *Polymer Composites* 9. 6 (1998): 443-452. Web.

Scott, D.W. “Thermal Rearrangement of Branched-Chain Methylpolysiloxanes.” *Journal of the American Chemical Society.* 68. (1946): 356. Web.

Silsesquioxanes: Bridging the Gap Between Polymers & Ceramics. (St. Louis: Sigma-Aldrich, 2001.

Siraki, A.G. et al. “N-Oxidation of Aromatic Amines by Intracellular Oxidases.” *Drug Metabolism Reviews.* 34. 3 (2002): 549-564. Web.

Strategic Environmental Research and Development Program. 2012. “Development of Replacements for Polyimide Composite Materials Containing Methylene Dianiline (MDA).” SON Number: WPSON-14-02. October 25, 2012. Web.

Tan, B.H. et al. “Tailoring Micell Formation and Gelation in (PEG-P(MA-POSS)) Amphiphilic Hybrid Block Copolymers.” *Macromolecules.* 44. 3 (2011): 622-631. Web.

Tandon, G.P. et al. 2007. “Thermo-oxidative behavior of High Temperature PMR-15 Resin and Composites.” Air Force Research Laboratory Report. AFRL-ML-WP-TP-2007-461. Web.

Tomczak, S.J. et al. 2005. “Properties and Improved Space Survivability of POSS (Polyhedral Oligomeric Silsesquioxane) Polyimides.” Materials Research Society Symposium Proceedings. 851. Web.

Uhl, K.M. et al. “Mechanical Strength Degradation of Graphite Fiber Reinforced Thermoset Composites Due to Porosity.” in *Review of Progress in Quantitative Nondestructive Evaluation*, edited by Thompson, D.O. and Chimenti, D.E., 1075-1082. New York: Springer US, 1988.

U.S. Department of Labor, “Occupational Exposure to 4,4’ Methylenedianiline (MDA).” 1910.19, 1910.1050, 1926.60.

Vij, V. et al. “Synthesis of Aromatic Polyhedral Oligomeric Silsesquioxane (POSS) Dianilines for Use in High-Temperature Polyimides.” *Silicon.* 4 (2012): 267-280. Web.

Watanabe, A. et al. “Hydrophobic Surface Based on Microtexture of Ag Nanoparticle/POSS Nanocomposite Film.” *Chemistry Letters.* 42.10 (2013): 1255-1256. Web.

Weinhold, F. and West, R. “The Nature of the Silicon-Oxygen Bond.” *Organometallics.* 30.1 (2011): 5815-5824. Web.

Wu, S. “Synthesis and Characterization of Semiaromatic Polyimides Containing POSS in Main Chain Derived from Double-Decker-Shaped Silsesquioxane.” *Macromolecules.* 40. (2007): 5698-5705. Web.

Yandek, G. 2013. “Non-toxic Multifunctional Silsesquioxane Diamine Monomer for Use in Aerospace Polyimides.” Strategic Environmental Research and Development Program Proposal 14 WP02-015. Print.

Yun, C.H. et al. “Contributions of Human Liver Cytochrome P450 Enzymes to the N-Oxidation of 4,4’-Methylene-Bis (2-Chloroaniline).” *Carcinogenesis*. 13. 2 (1992): 217-222. Web.